Seismic induced flooding

- **Failure of sprinkler head**

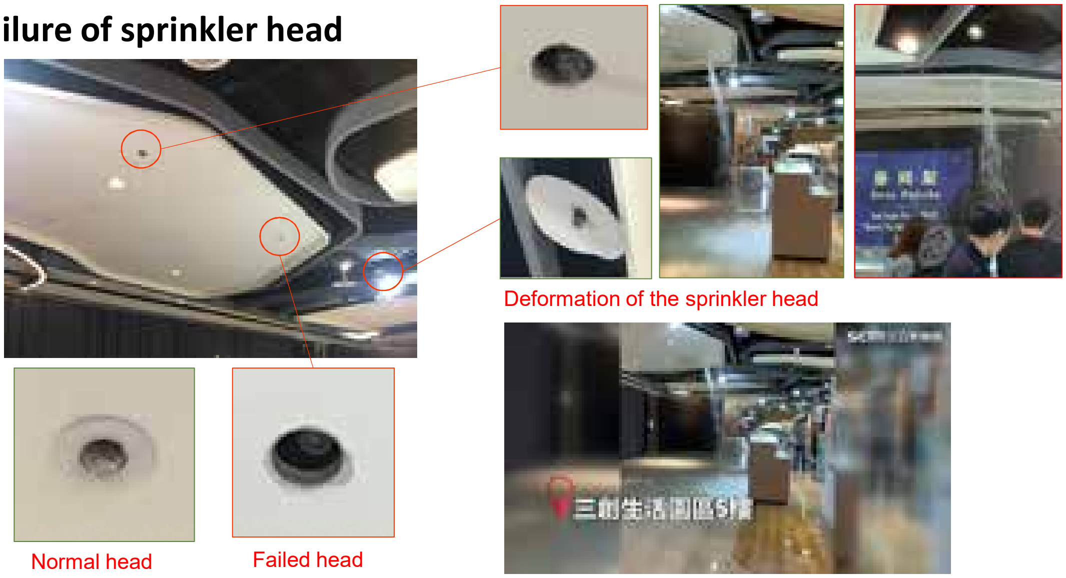

Deformation of the sprinkler head

Normal head

Failed head

Procedures for Fragility Analysis

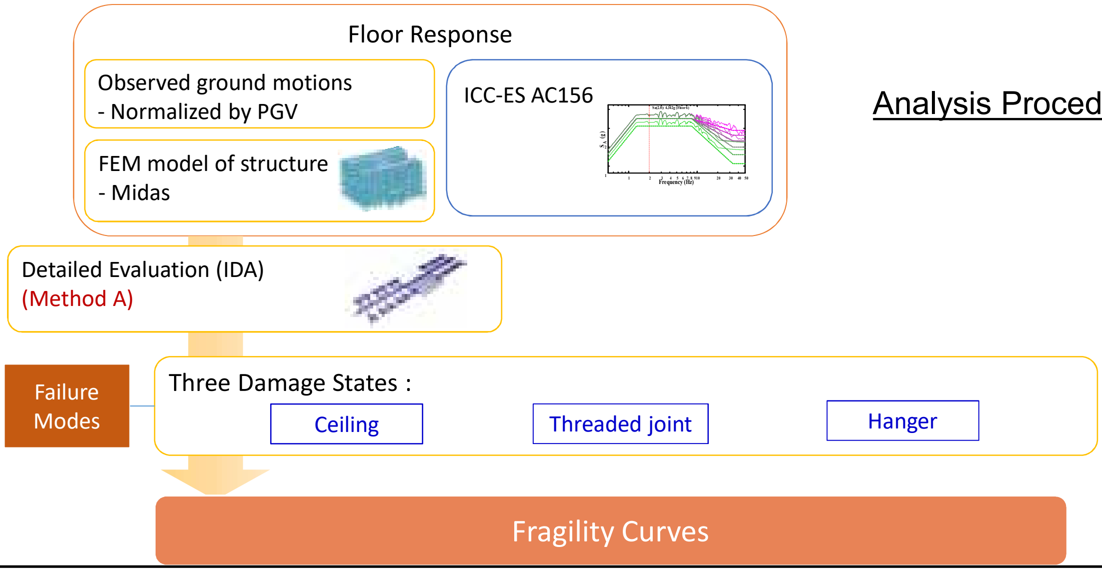

Floor Response

Observed ground motions
- Normalized by PGV

FEM model of structure
- Midas

ICC-ES AC156

Detailed Evaluation (IDA)
(Method A)

Failure Modes

Three Damage States :

Ceiling

Threaded joint

Hanger

Fragility Curves

Analysis Procedures

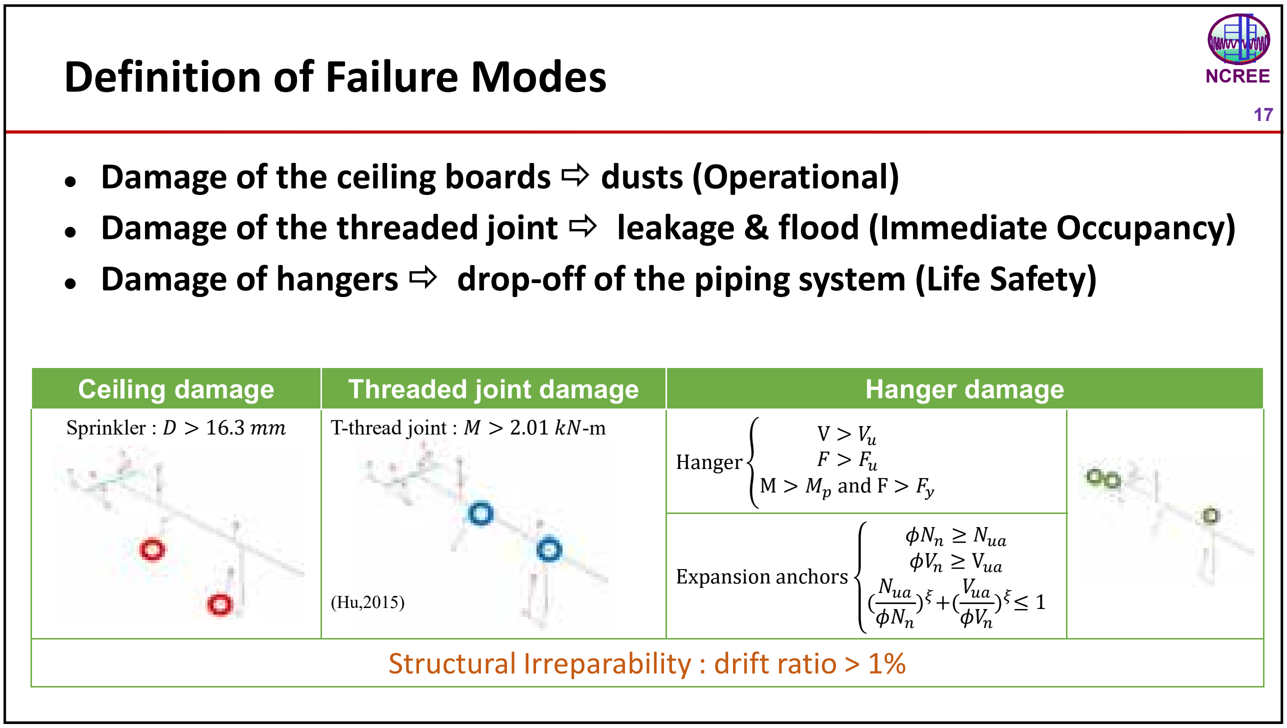

Definition of Failure Modes

- Damage of the ceiling boards ⇨ dusts (Operational)
- Damage of the threaded joint ⇨ leakage & flood (Immediate Occupancy)
- Damage of hangers ⇨ drop-off of the piping system (Life Safety)

Ceiling damage	Threaded joint damage	Hanger damage
Sprinkler : $D > 16.3\ mm$	T-thread joint : $M > 2.01\ kN$-m (Hu,2015)	Hanger $\begin{cases} V > V_u \\ F > F_u \\ M > M_p \text{ and } F > F_y \end{cases}$ Expansion anchors $\begin{cases} \phi N_n \geq N_{ua} \\ \phi V_n \geq V_{ua} \\ (\frac{N_{ua}}{\phi N_n})^{\xi} + (\frac{V_{ua}}{\phi V_n})^{\xi} \leq 1 \end{cases}$
Structural Irreparability : drift ratio > 1%		

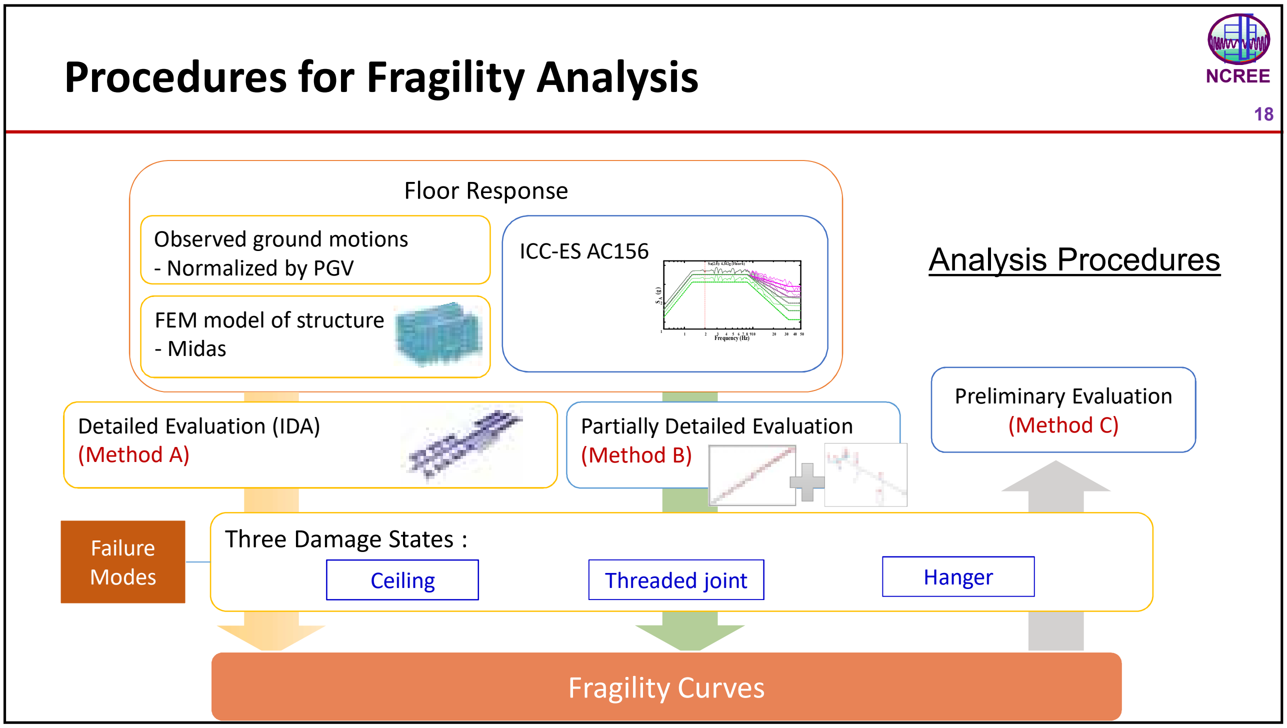

Procedures for Fragility Analysis

Floor Response

Observed ground motions
- Normalized by PGV

FEM model of structure
- Midas

ICC-ES AC156

Analysis Procedures

Detailed Evaluation (IDA)
(Method A)

Partially Detailed Evaluation
(Method B)

Preliminary Evaluation
(Method C)

Failure Modes

Three Damage States :

Ceiling

Threaded joint

Hanger

Fragility Curves

Preliminary Evaluation—Method C (1/4)

- **Frequency of the piping system**

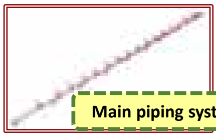

Main piping system

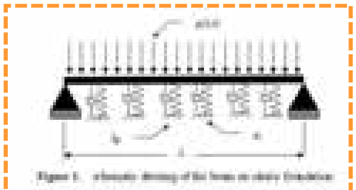

Salih N Akour (2012)

$$k = \frac{3EI}{L^3} \rightarrow K_f = \sum_{i=1}^{n} k_i$$

①

Mass from Diameter and length of the piping system ②

$$\omega^2 = \omega_1^2 + \omega_f^2$$

$$\omega_f^2 = \frac{K_f}{M}, \quad \omega_1 = (\beta_1 l)^2 \sqrt{\frac{EI}{Ml^3}}$$

③

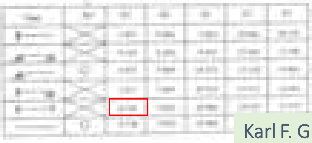

Karl F. Graff (1985)

ω_1: ***Frequency due to B.C. of main pipe***

ω_f: ***Frequency due to Hangers (Parallel connection)***

Preliminary Evaluation—Method C (2/4)

- **Displacement Response of Main Piping System**
  - **Estimated from spectral displacement at piping frequency**

$$\Delta_{main\ pipe} = MF_1 \times S_d(pipe\ f)$$

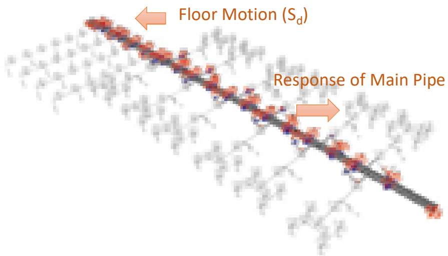

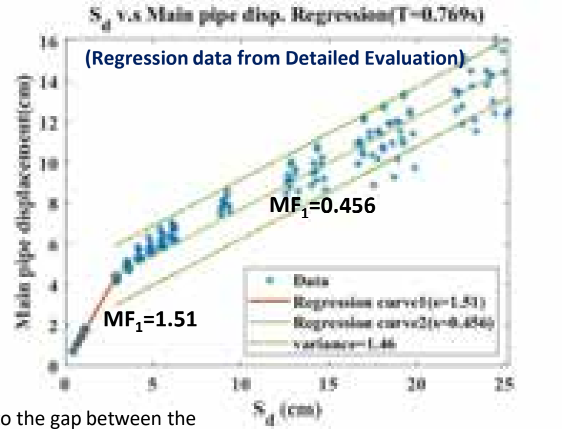

Bilinear: Due to the gap between the sprinkler piping and partition walls

Preliminary Evaluation—Method C (3/4)

- **Seismic Demand for Each Failure Mode**
  - **Estimated from displacement response of main piping system**

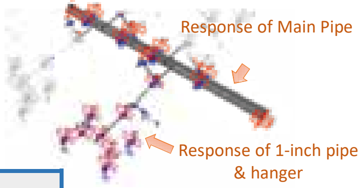
Response of Main Pipe
Response of 1-inch pipe & hanger

Displacement of sprinkler heads

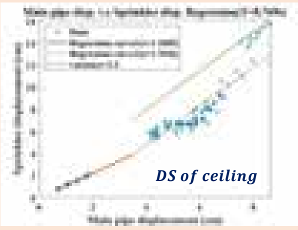

$\Delta_{head} = MF_2(\Delta_{main}) \cdot \Delta_{main}$

Bilinear regression formula

Leakage of 1" threaded joint

Moment at threaded joint = $K_r\theta$

where $\theta = (\Delta_{Main\ pipe} - \Delta_{gap}) / L$

L = length between partition wall & threaded joint

K_r = rotational stiffness of threaded joint

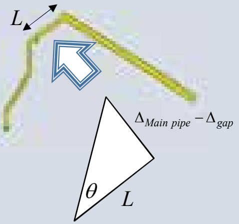
L
$\Delta_{Main\ pipe} - \Delta_{gap}$
θ
L

CP stage of hanger

$$\text{Moment at hanger} = \frac{3EI\Delta_{main\ pipe}}{L^2_{hanger}}$$

$$\text{Shear Force} = M/L_{hanger}$$

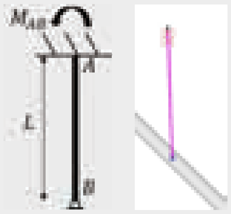

Preliminary Evaluation—Method C (4/4)

- **Application Procedure**

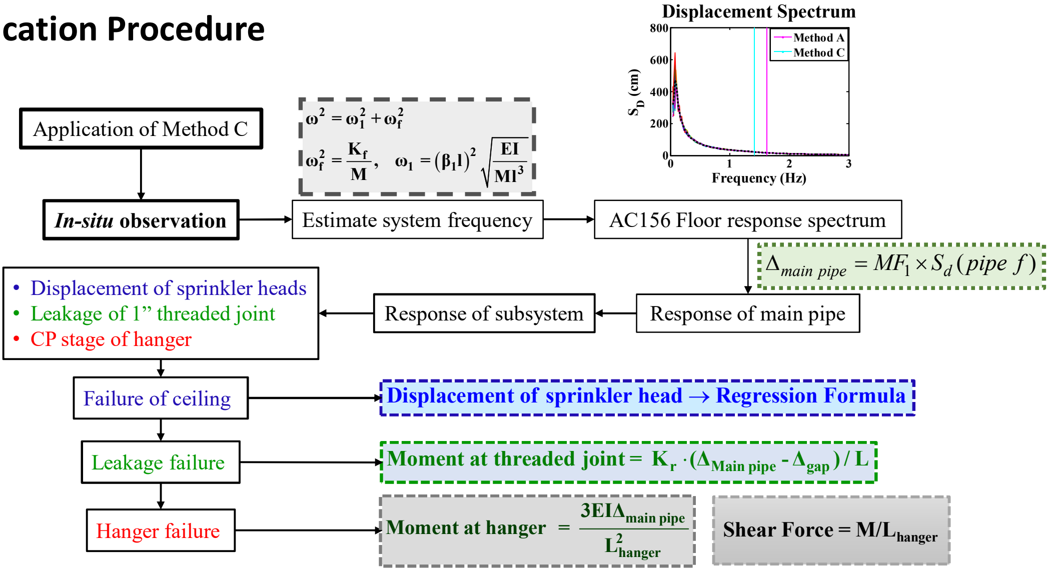
Displacement Spectrum
S_D (cm)
800
600
400
200
0
0
1
2
3
Frequency (Hz)
Method A
Method C

Application of Method C

$\omega^2 = \omega_1^2 + \omega_f^2$

$\omega_f^2 = \frac{K_f}{M}, \quad \omega_1 = (\beta_1 l)^2 \sqrt{\frac{EI}{Ml^3}}$

***In-situ* observation**

Estimate system frequency

AC156 Floor response spectrum

$\Delta_{main\ pipe} = MF_1 \times S_d(pipe\ f)$

Response of main pipe

Response of subsystem

- Displacement of sprinkler heads
- Leakage of 1" threaded joint
- CP stage of hanger

Failure of ceiling → **Displacement of sprinkler head → Regression Formula**

Leakage failure → **Moment at threaded joint = $K_r \cdot (\Delta_{Main\ pipe} - \Delta_{gap}) / L$**

Hanger failure → **Moment at hanger = $\frac{3EI\Delta_{main\ pipe}}{L^2_{hanger}}$** **Shear Force = M/L_{hanger}**

Comparison of Fragility Curves

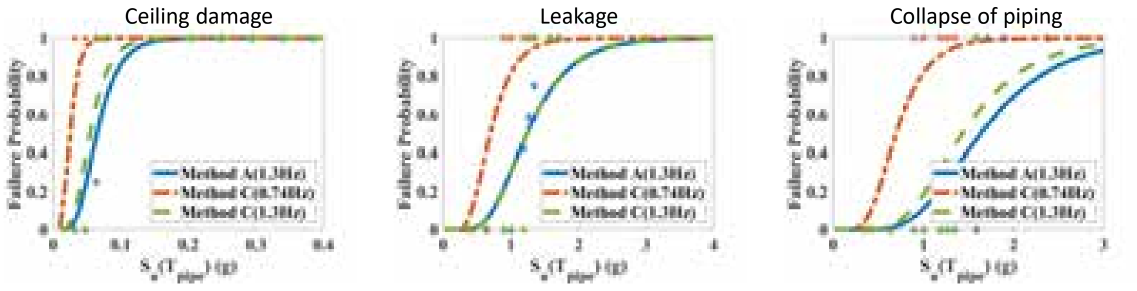

Compare the leakage and collapse fragility curves with FEMA P58

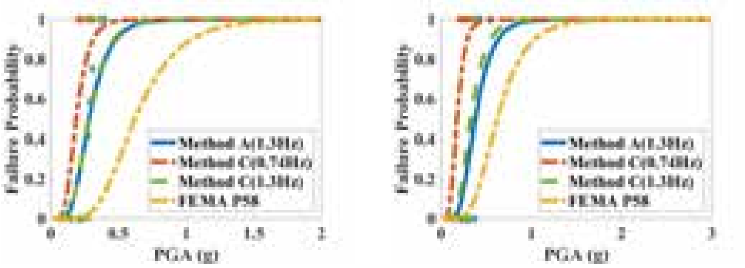

Strengthen Strategy of Sprinkler Piping System

- **NFPA 13**
  - ✓ Install bracing on main pipe (Chai et al. , 2015)
  - ✓ Install bracing on branch pipe
  - ✓ Install #12 Splay wires on Sprinkler heads

Not effectively decrease the disp. of the sprinkler head

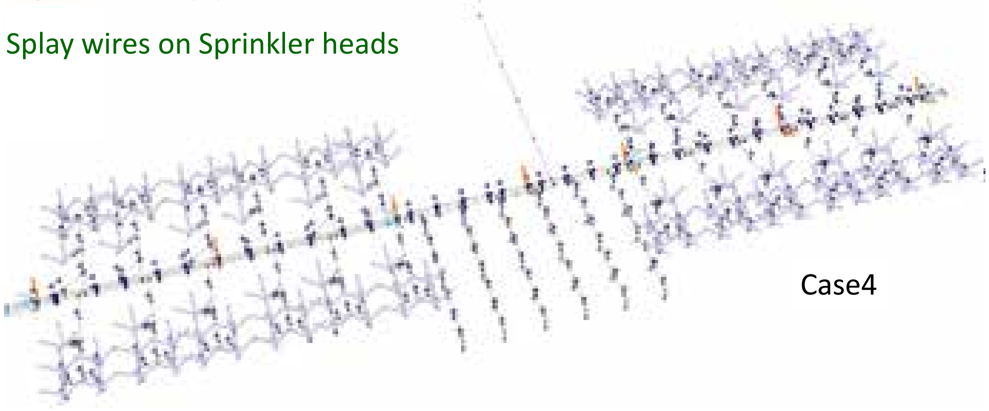

Shaking Table Test in October, 2019

NCREE

- Test Configuration

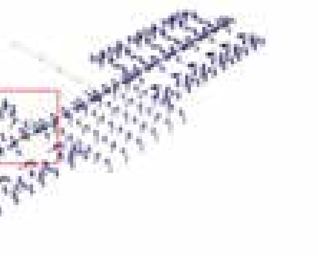

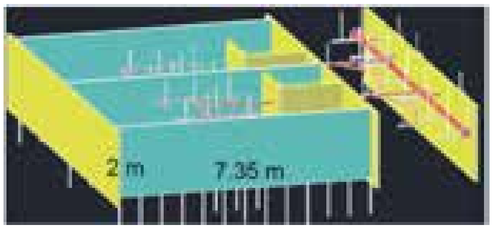

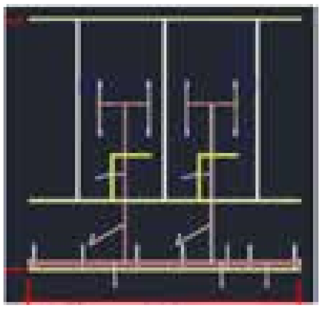

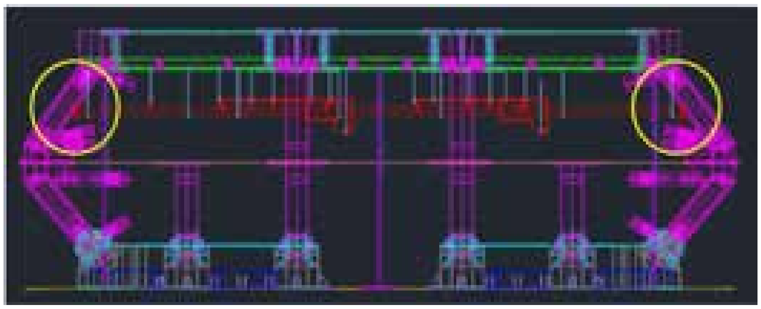

NARLabs

Near-fault Effect on Convective Mode of Storage Liquid in Tanks

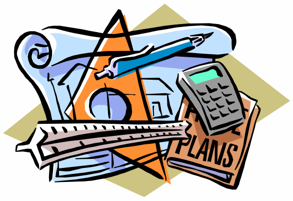

Introduction

- **Period for Convective Mode**
  - **ACI 350.3-06**

$$T_c = \left(\frac{2\pi}{\lambda}\right)\sqrt{D} \quad \text{with} \qquad \lambda = \sqrt{3.68g\tanh\left[3.68\left(\frac{H_L}{D}\right)\right]}$$

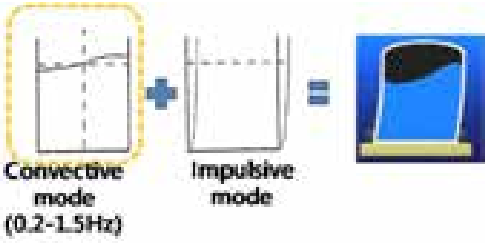
Convective mode (0.2-1.5Hz)
Impulsive mode

- **Sloshing Height (for circular tank)**
  - **ACI:** $h_s = IR\left(\frac{S_a}{g}\right)$
  - **SPID:** $h_s = 1.2 * IR\left(\frac{S_a}{g}\right)$
  - **GIP-3A:** $h_s = 0.837R\left(\frac{S_a}{g}\right)$

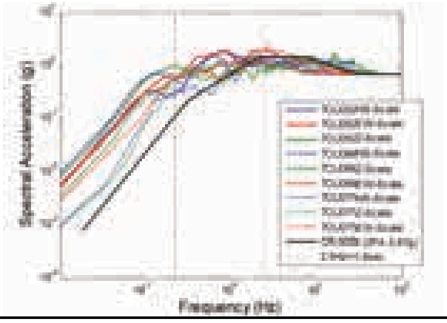

Input Motions

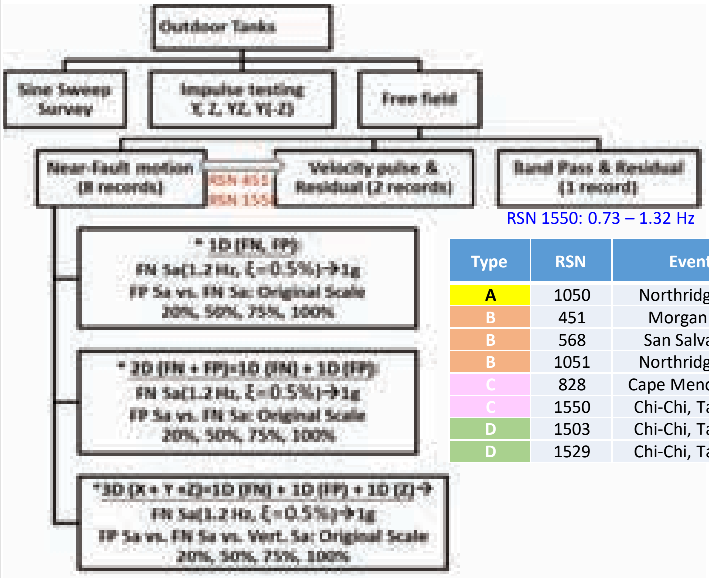
Outdoor Tanks
Sine Sweep Survey
Impulse testing Y, Z, YZ, Y(-Z)
Free field
Near-Fault motion (8 records)
RSN 451
RSN 1550
Velocity pulse & Residual (2 records)
Band Pass & Residual (1 record)
* 1D (FN, FP)
FN Sa(1.2 Hz, ξ=0.5%)→1g
FP Sa vs. FN Sa: Original Scale
20%, 50%, 75%, 100%
* 2D (FN + FP)=1D (FN) + 1D (FP)
FN Sa(1.2 Hz, ξ=0.5%)→1g
FP Sa vs. FN Sa: Original Scale
20%, 50%, 75%, 100%
*3D (X + Y +Z)=1D (FN) + 1D (FP) + 1D (Z)→
FN Sa(1.2 Hz, ξ=0.5%)→1g
FP Sa vs. FN Sa vs. Vert. Sa: Original Scale
20%, 50%, 75%, 100%

RSN 1550: 0.73 – 1.32 Hz

Type	RSN	Event	Station	T_P (sec)	T_{Sv} (sec)
A	1050	Northridge-01	Pacoima Dam (downstr)	0.504 << 0.8	0.445 << 0.8
B	451	Morgan Hill	Coyote Lake Dam (SW Abut)	0.952 ~= 0.8	0.688 ~= 0.8
B	568	San Salvador	Geotech Investig Center	0.861 ~= 0.8	0.647 ~= 0.8
B	1051	Northridge-01	Pacoima Dam (upper left)	0.896 ~= 0.8	0.733 ~= 0.8
C	828	Cape Mendocino	Petrolia	2.996 >> 0.8	0.733 ~= 0.8
C	1550	Chi-Chi, Taiwan	TCU136	10.326 >> 0.8	0.940 ~= 0.8
D	1503	Chi-Chi, Taiwan	TCU065	5.740 >> 0.8	4.453 >> 0.8
D	1529	Chi-Chi, Taiwan	TCU102	9.723 >> 0.8	2.543 >> 0.8

Test Configuration

- **Instrument Configuration**
  - **Water level: measured by Temposonic**
    - ✓ **Magnet ring inside a buoy up-and-down along the sensing rod**

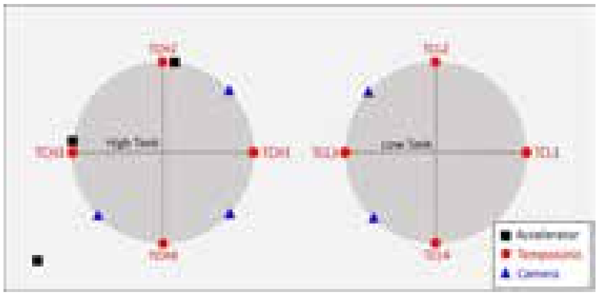
TCH2
TCH3
High Tank
TCH1
TCH4
TCL2
TCL3
Low Tank
TCL1
TCL4
Accelerometer
Temposonic
Camera

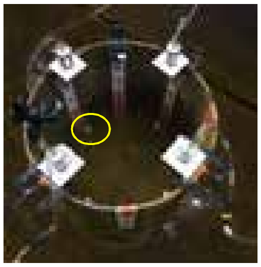

Preliminary Results (1/4)

- **Natural Frequencies of Tanks**

Test Results

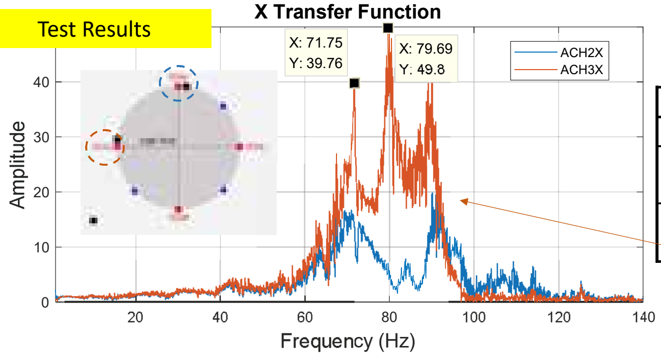

Numerical Results

Circular tanks			
Set	Tank heights (m)	Thickness (m)	Frequencies of 1st mode(Hz)
1	0.5	0.0103	364.96
	1	0.0103	181.28
2	0.7	0.0103	272.16
	1.2	0.0103	141.16

Much higher than the frequencies of sloshing modes

⇒ Effect of impulse mode may be neglected

Preliminary Results (2/4)

- **Natural Frequency of Convective Mode**

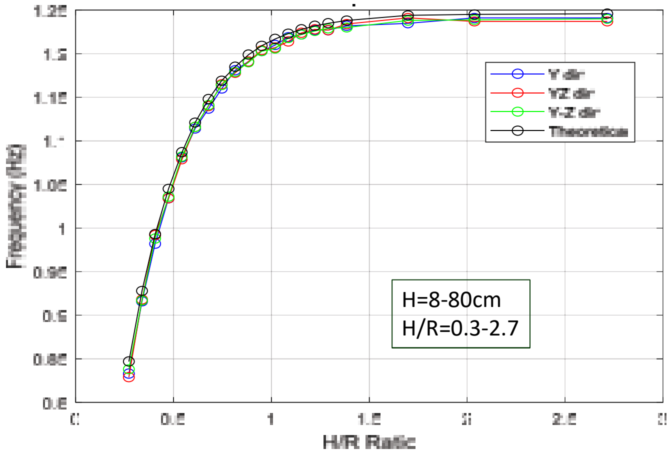

THE RELATIONSHIP BETWEEN SLOSHING FREQUENCY AND *H*/*R*

$$T_c = \left(\frac{2\pi}{\lambda}\right)\sqrt{D}$$

$$\lambda = \sqrt{3.68g\tanh\left[3.68\left(\frac{H_L}{D}\right)\right]}$$

The effect of vertical input on the sloshing frequency is not so significant.

Preliminary Results (3/4)

- **Damping Ratio of Convective Mode**

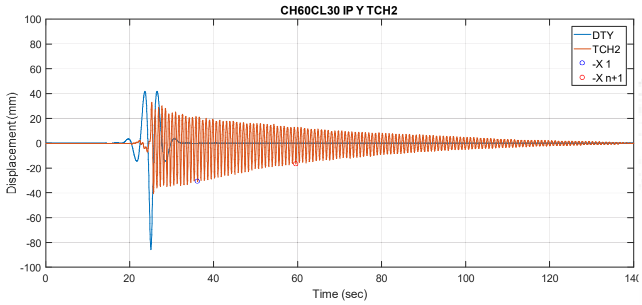

Impulse test: ch60cl30_ip_y_tch2

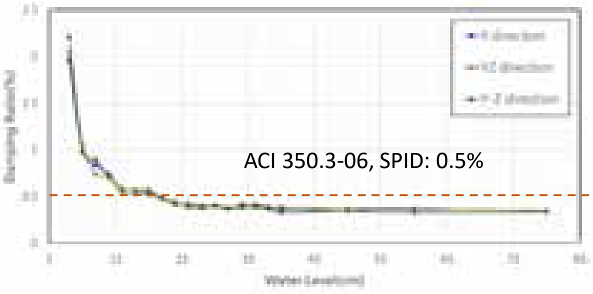

ACI 350.3-06, SPID: 0.5%

- The damping ratio decrease dramatically while the water level increases from 8cm to 15cm
- The damping ratio is converged to about 0.4%

logarithmic decrement damping ratio

$$\delta = \frac{1}{n} ln\left|\frac{X_1}{X_{n+1}}\right| \Rightarrow \xi = \frac{\delta}{\sqrt{4\pi^2+\delta^2}}$$

Preliminary Results (4/4)

NCREE

- **Sloshing Height**
  - **1D**
  - **2D**

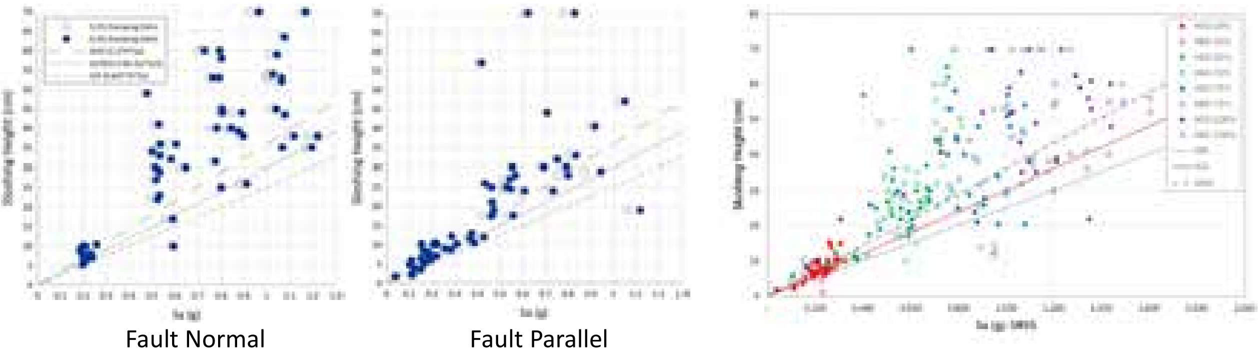

Fault Normal

Fault Parallel

SPID (1.2*R*Sa)
ACI350.3-06 (Sa*D/2)
GIP (0.837*R*Sa)

$$S_a = \sqrt{S_{ax}^2 + S_{ay}^2}$$

Future Works

Possible relationship between parameters of input motions and sloshing height / splashing volume

NCREE

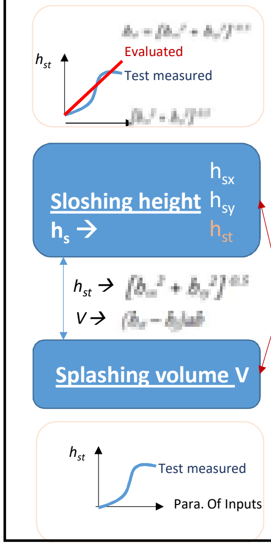

Convective Period T_s(tested)

Para. Of Inputs

Damping ratio 0.4% (tested)

$h_s = 0.837\ R\ Sa$ [illegible]

1. Spectral Acc. $S_a(T_s)$
   1. Effects of multi-direction inputs: Uni-axial , Bi-axial, Tri-axial
   2. Effects of frequency content of inputs [BP vs. RBP]
2. Spectral Velocity $S_v(T_s)$
3. Spectral Displacement $S_d(T_s)$
4. Convective Period T_s vs. Significant Period of Input motion T_a (FFT)→ T_s/T_a
5. Convective Period T_s vs. Pulse period of Input motion T_p → T_s/T_p
   1. Resonance effects of T_p and T_s [VP vs. RVP]
6. Comparing Effects of T_s and T_p [VP vs. BP]
7. Convective Period T_s vs. Significant Period of Input Spectral Acc. Ts_a → T_s/Ts_a
8. Convective Period T_s vs. Significant Period of Input Spectral Vel. Ts_v → T_s/Ts_v
9. Convective Period T_s vs. Significant Period of Input Spectral Dis. Ts_d → T_s/Ts_d
10. RMS of Input Acceleration
11. Cumulative Energy E(t), Total Energy E_t
12. Power P(t)=dE(t)/dt, max. Power P_m
13. Duration of Strong motion D [Tp~= 0.8 sec]
14. Stress Cycle Number C_n

Tp~= 0.8sec

Tp>>0.8sec

Tp<<0.8sec

TpWave>>0.8sec,
TpSv~=0.8sec

RSN	Original Event
1051	Northridge-01
1529	Chi-Chi, TCU102
568	San Salvador
1503	Chi-Chi, TCU065
1050	Northridge-01
1550	**Chi-Chi, TCU136**
828	Cape Mendocino
451	Morgan Hill

RSN	Input Type
1550	Original VP, RVP BP, RBP
451	Original VP, RVP FW

THANK YOU FOR YOUR ATTENTION

Speaker: Dr. Juin-Fu Chai

Email: chai@ncree.narl.org.tw

NON-STRUCTURAL RESEARCH IN SUSPENDED CEILING AND STATIC SMOKE BARRIER SYSTEM

By Dr. G.C. Yao, National Cheng Kung University

Abstract

The seismic performance of suspended non-structural elements is generally poor if the suspension length is large and there is no mechanism to prevent collision or detachment. The most vivid examples are suspended ceiling. If suspended ceilings were to be provided with adequate strengthening mechanism against earthquake, such as the ones prescribed in ASTM E580, the laboratory performance usually proved excellent. However, the bracing requirement in ASTM E580 is a major construction headache because of piping/ducking systems above the ceiling panels become obstacles for bracing installation.

We conducted research on seismic strengthening systems for several years and tested samples of small area ceiling systems and finally in 2018 conducted a large scale (10m ×10m) testing on ceiling systems with 3 configurations to check the ceiling's seismic performance. Together with the test, we also tested the smoke barrier (SB) systems that are usually attached to ceiling panels' underside. SB glass panels are easy to break in earthquakes and hence reduced the fire capacity of the building in post-earthquake fire. We tested SB improvement methods and found some inexpensive improvement technique effective.

This presentation will describe the researches on suspended ceiling and SB in the past few years in Taiwan and also discuss some of the findings and their engineering significance.

Keywords: suspended ceiling, smoke barrier, shaking table testing, numerical simulation.

Biography

Dr. George C. Yao is a Professor in Department of Architecture of NCKU in southern Taiwan. His professional experiences include working for a famous architectural firm (JP&A) and CALTRANS in the United States. His research encompasses various fields in the earthquake engineering in both structural behavior and nonstructural elements and has published numerous papers. In the past decade, his research interests expand into the disaster resilient buildings for flooding.

Joint NRC-MOST Workshop-Earthquake Engineering Technologies

NS Research in Suspended Ceiling and SSB System

2019/10/08

George Yao
Prof. Dept. Architecture,
NCKU

Fallen Ceilings in EQ

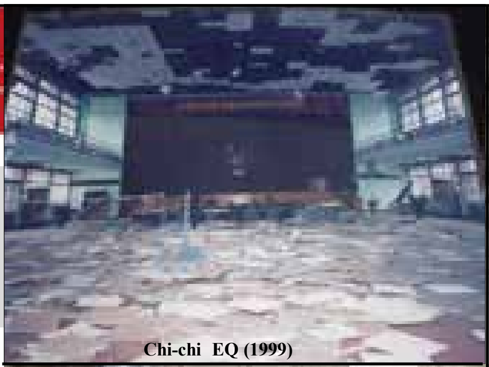

Chi-chi EQ (1999)

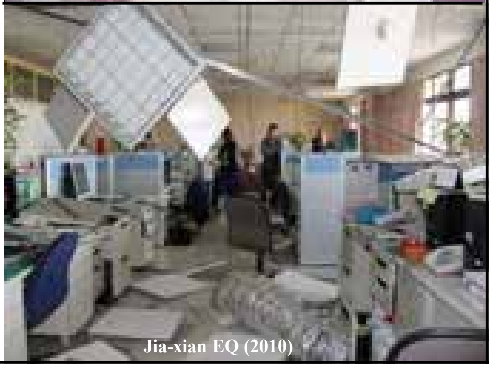

Jia-xian EQ (2010)

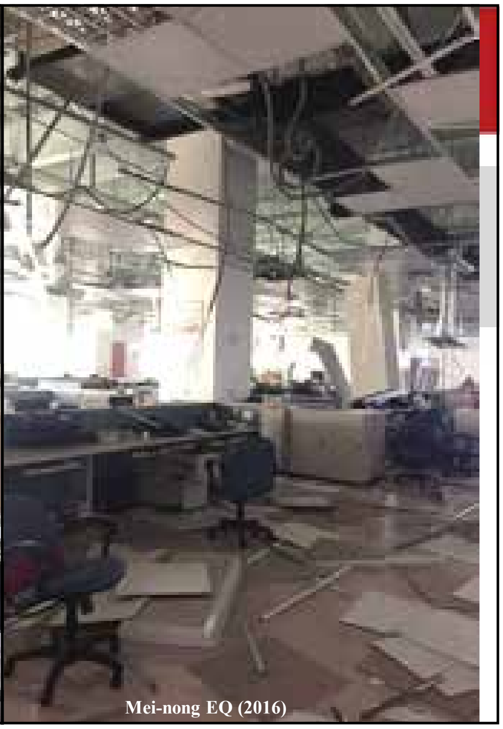

Mei-nong EQ (2016)

Background

Taiwan Bldg code require EQ-Res Susp. Ceiling (2010)

- ASTM E580
  - Runner connection strength above 80 kgf
  - Bracing Assembly (BA): 4 wires + 1 comp. post

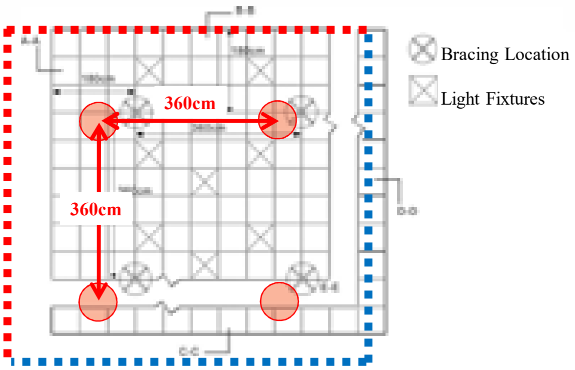
B-B
A-A
180cm
360cm
360cm
D-D
E-E
C-C
Bracing Location
Light Fixtures

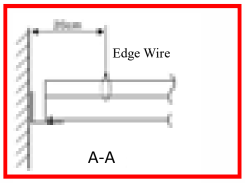
Edge Wire
A-A

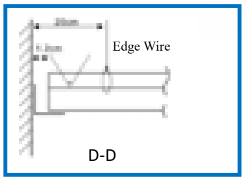
Edge Wire
D-D

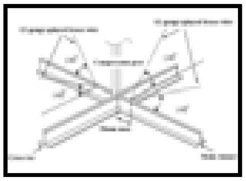

BA construction is challenging at field

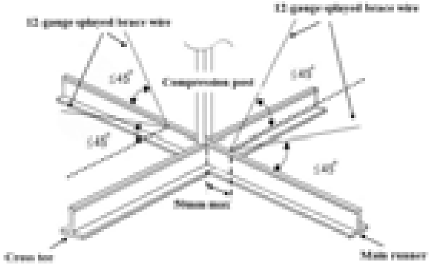
12 gauge splayed brace wire
12 gauge splayed brace wire
Compression post
≤45°
≤45°
≤45°
≤45°
Main runner
Cross tee
Main runner

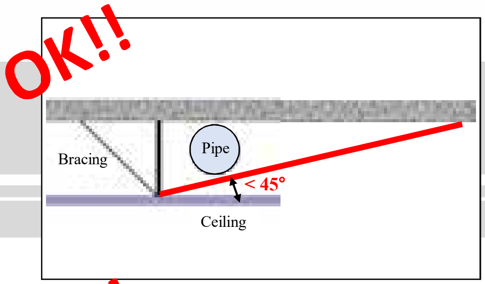
OK!!
Bracing
Pipe
< 45°
Ceiling

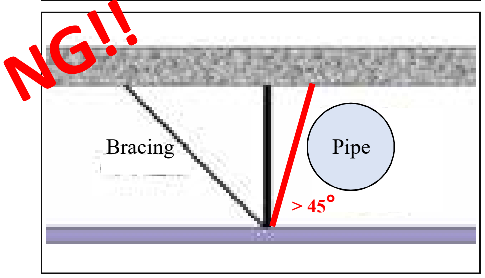
NG!!
Bracing
Pipe
> 45°

EQ performance w/o BA (2016)

Mei-nong EQ (2016)	Yujing Farmers' Association
Ceiling Area	676.35m^2
Ceiling System	Unbraced Ceiling
Ceiling Grid	Seismic Runner
Location	4F
PGA	400gal

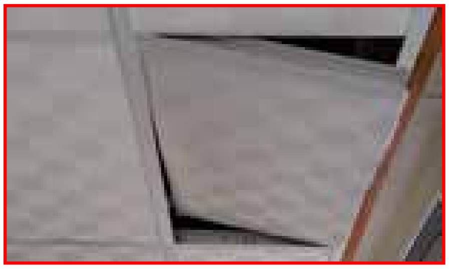

Unbraced Ceiling

Experiment in NCREE (2015)

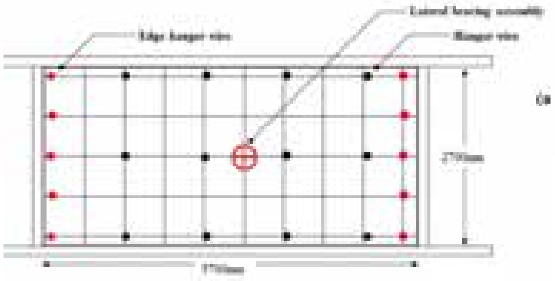
Lateral bracing assembly
Edge hanger wire
Hanger wire
(a)
2770mm
5770mm

Ceiling Size:5.7 m × 2.7 m

Experimental Analysis

C1: Sin-H800

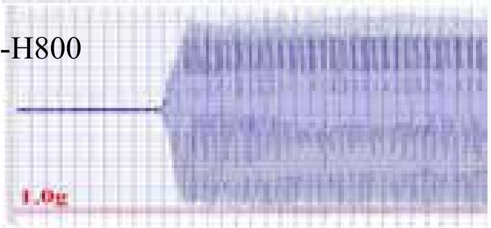

Response acceleration of the ceiling

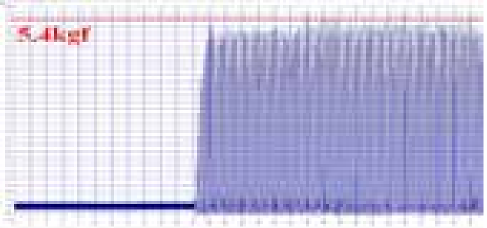

Tensile force of the splayed wire

Self-weight of ceiling :165kgf,
Inertial force ~ 165kgf.

5.4/165=0.033=3.3%

Experimental Analysis (Chi-Chi EQ)

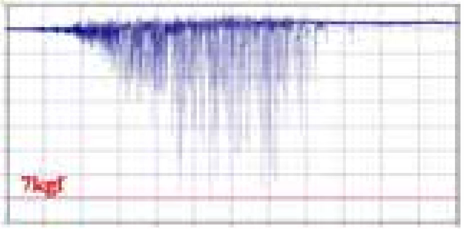

Tensile force of the splayed wire on C9

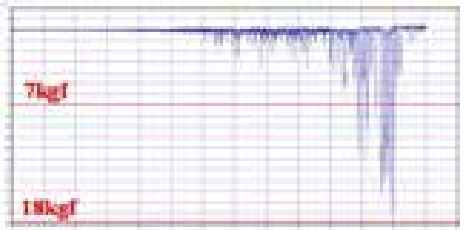

Tensile force of the splayed wire on C10

Test Series	Specimen	Config.	Bracing Assembly	Input Direction	Peak Acceleration	
					H	V
2	C9	C	Yes	X	1.3 g	0 g
	C10	C	Yes	X+Z	1.3 g	1.3 g

In comparison with the result of C9, the splayed wire of C10 sustained more tensile force. However, the maximum tensile force measured before the ceiling collapsed is 18kgf, which indicates that the bracing wire still sustains less than 10% of the horizontal inertial force.

Preliminary Conclusions in 2015

- **Seismic ceiling shows good resistance to Horizontal motion.**
- **In BA, brace wires carry little loads**
  - Inertia force mainly carried to the fixed edges on runners
- **The necessity of BA in seismic ceiling is in doubt.**

Large Scale Experiment (2019)

Suspension Frame Area: 12 X 12 m

Tested Ceiling Layout

Armstrong Product:

Peak Form: PRELUDE XL
Main Runner Ht:43 mm (BP734043)

Only Runners and Ceiling Panels

Ceiling Area: 10 X 10 m
Installed to ASTM E580

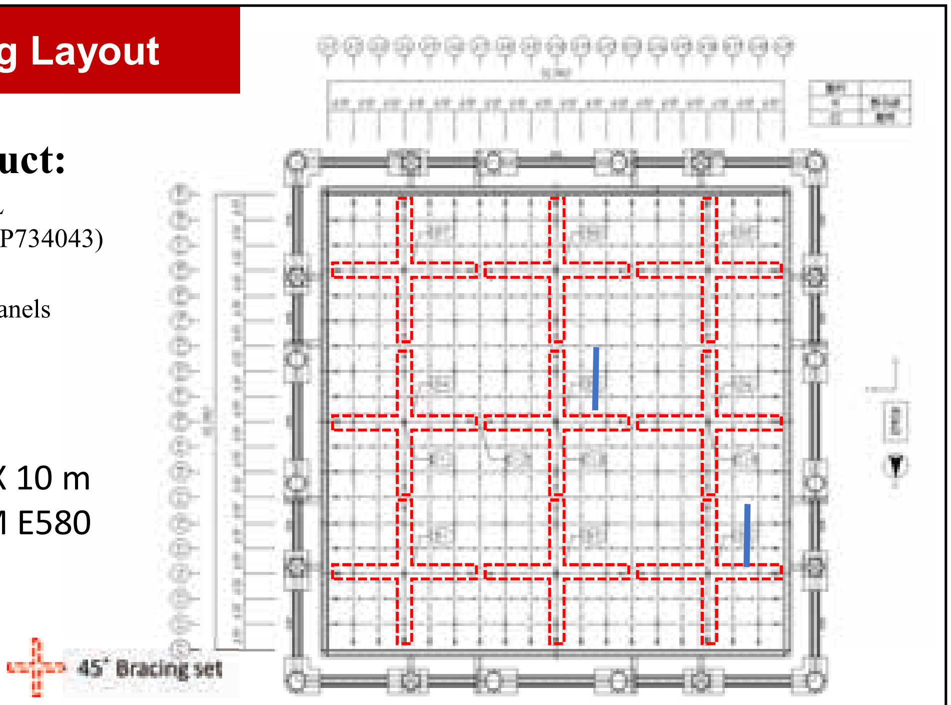
45° Bracing set

Tested Types

Suspension Height: 158 cm

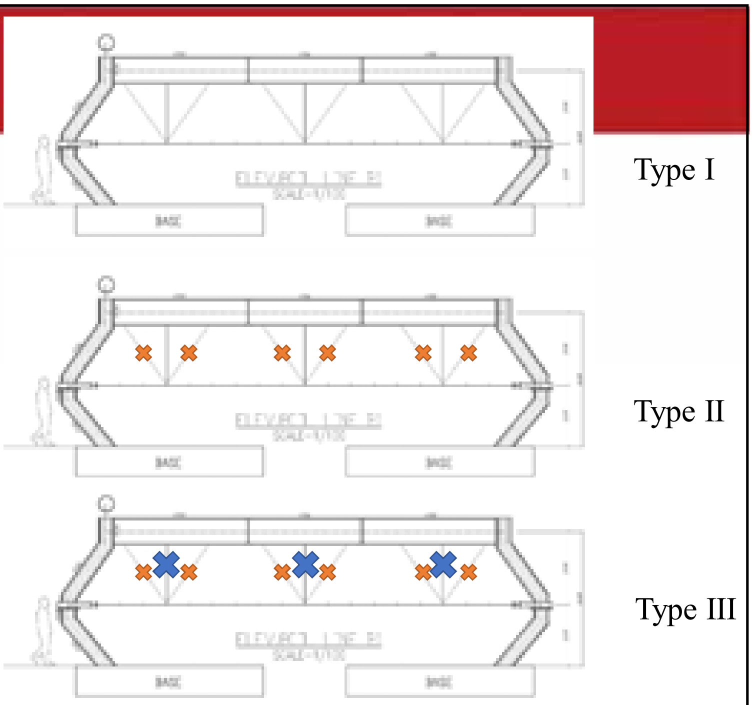
Type I
Type II
Type III

Bracing Force in 1 Hz Excitation

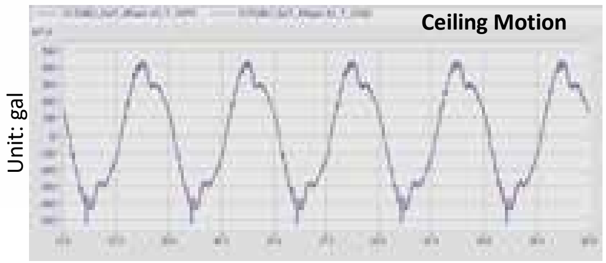

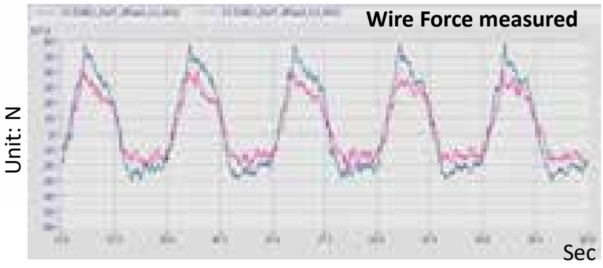

PA=0.45 g
Total Mass=461 kgm
Lateral Force= 0.45 g x 461 kgm=207 kgf

Lateral Force from Central Bracing=$6\ kgf \times \frac{\sqrt{2}}{2} = 4.24\ kgf$

Lateral Force from Corner Bracing=$4\ kgf \times \frac{\sqrt{2}}{2} = 2.83\ kgf$

Total Lateral Force Support By Bracing=
$4.24 \times 3 + 2.83 \times 6 = 29.70\ kgf$

Bracing Participation Ratio= 207 kgf / 29.70 kgf =14.31%

Excitation motions

AC 156

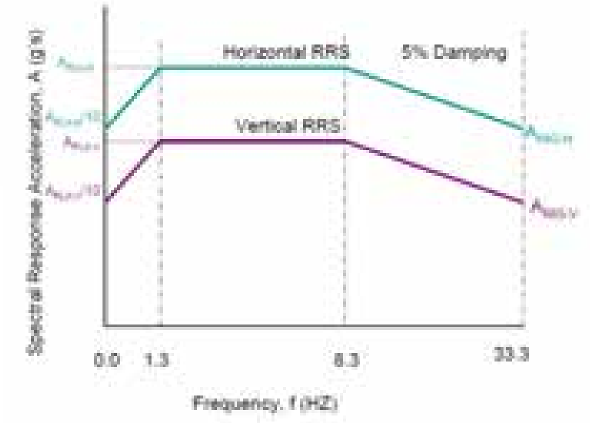

Max S_{DS} in Taiwan is 0.96 g

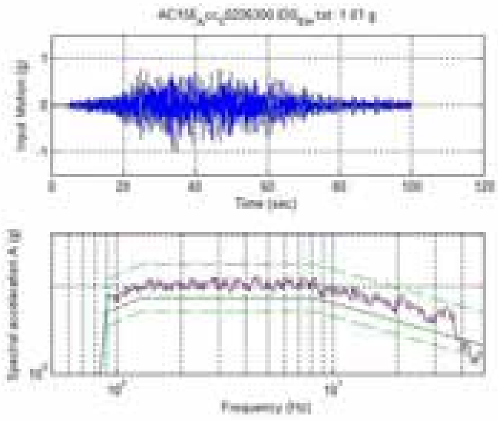

Test Results

- No Falling Objects in Type I, II, III
- Different Damage patterns at peripheral edges
  - Different Load transfer path in Type I, II, III

Type I	**Type III**
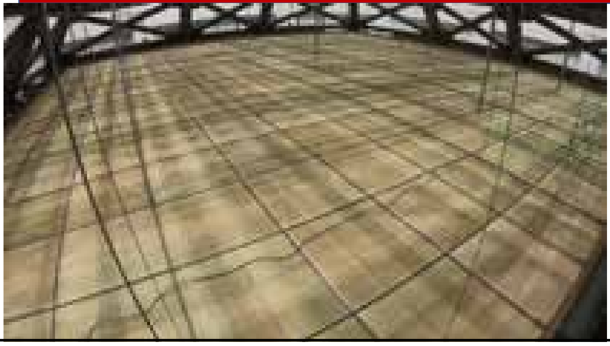	

Damage Pattern # at edges

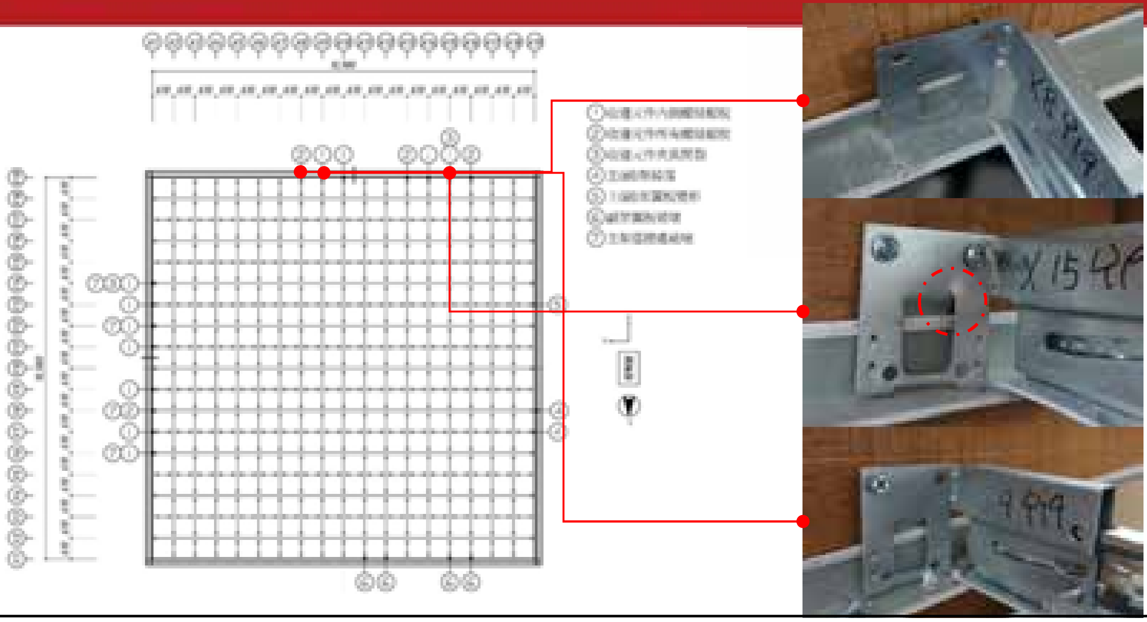

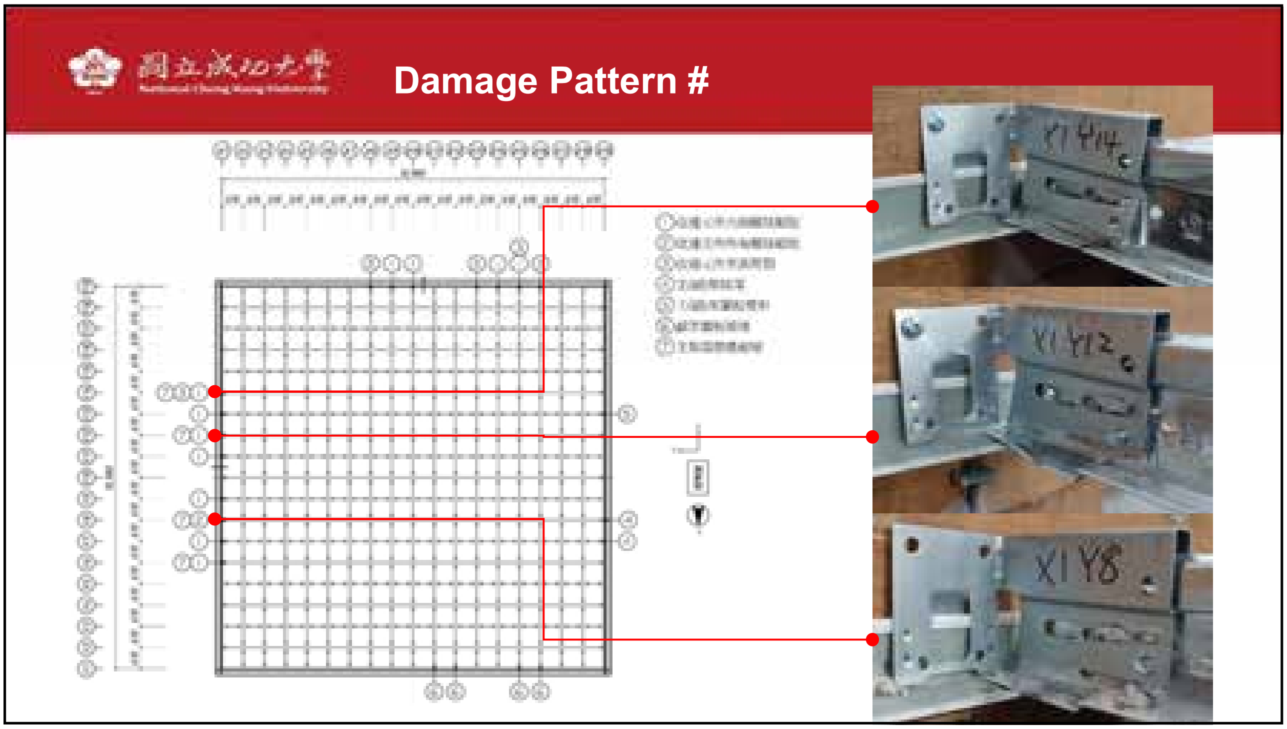

國立成功大學
National Cheng Kung University

Damage Pattern

X1Y14
X1Y12
X1Y8

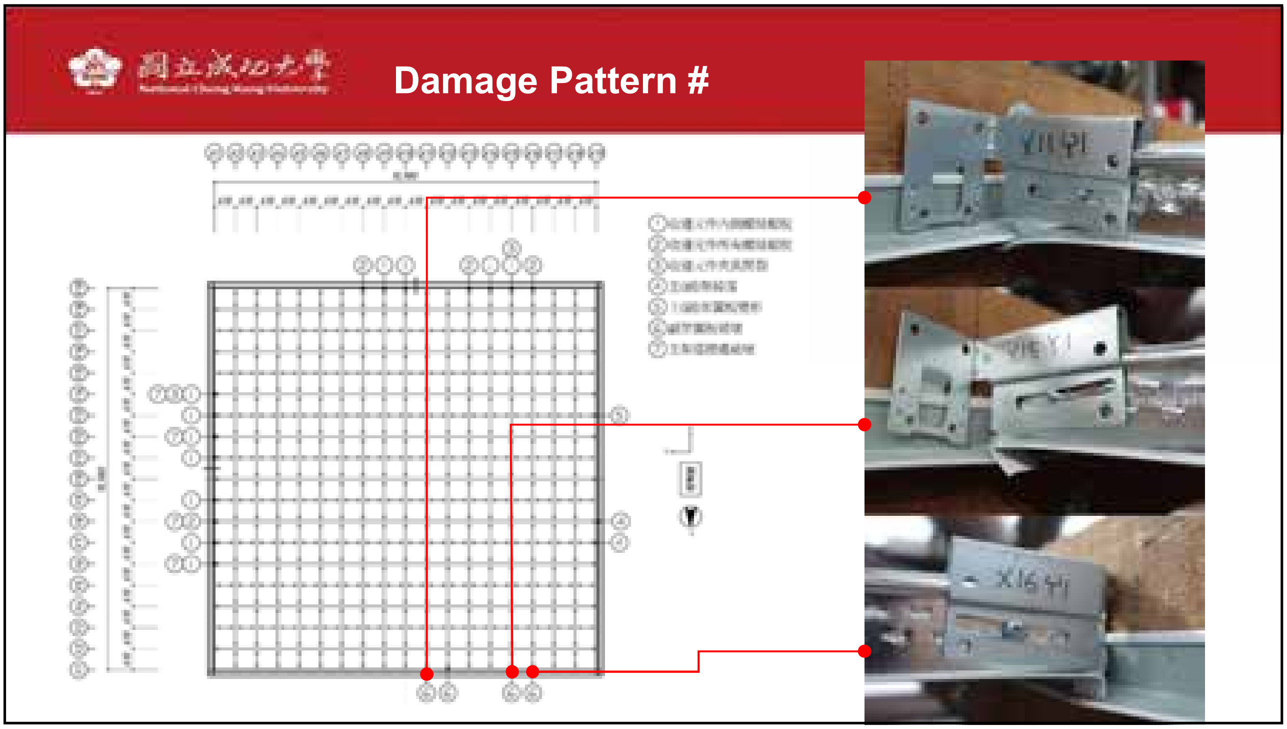

國立成功大學
National Cheng Kung University

Damage Pattern

X11Y1
X16Y1

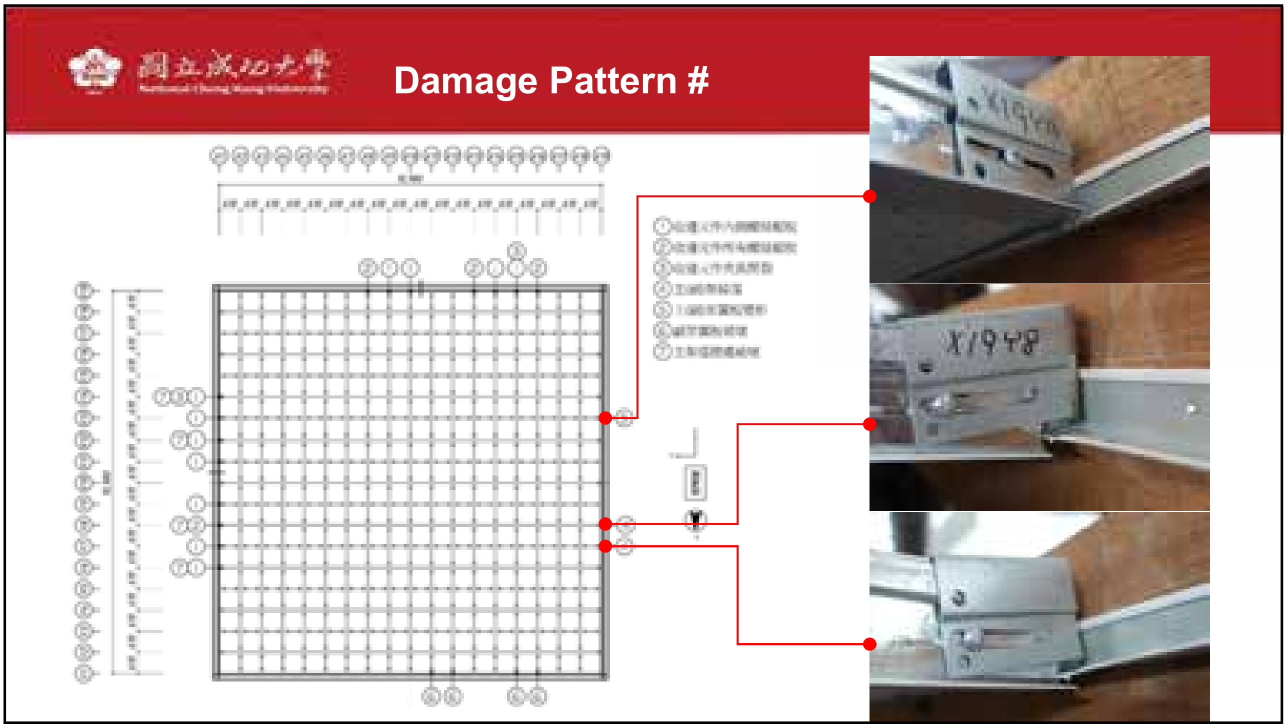

Damage Pattern

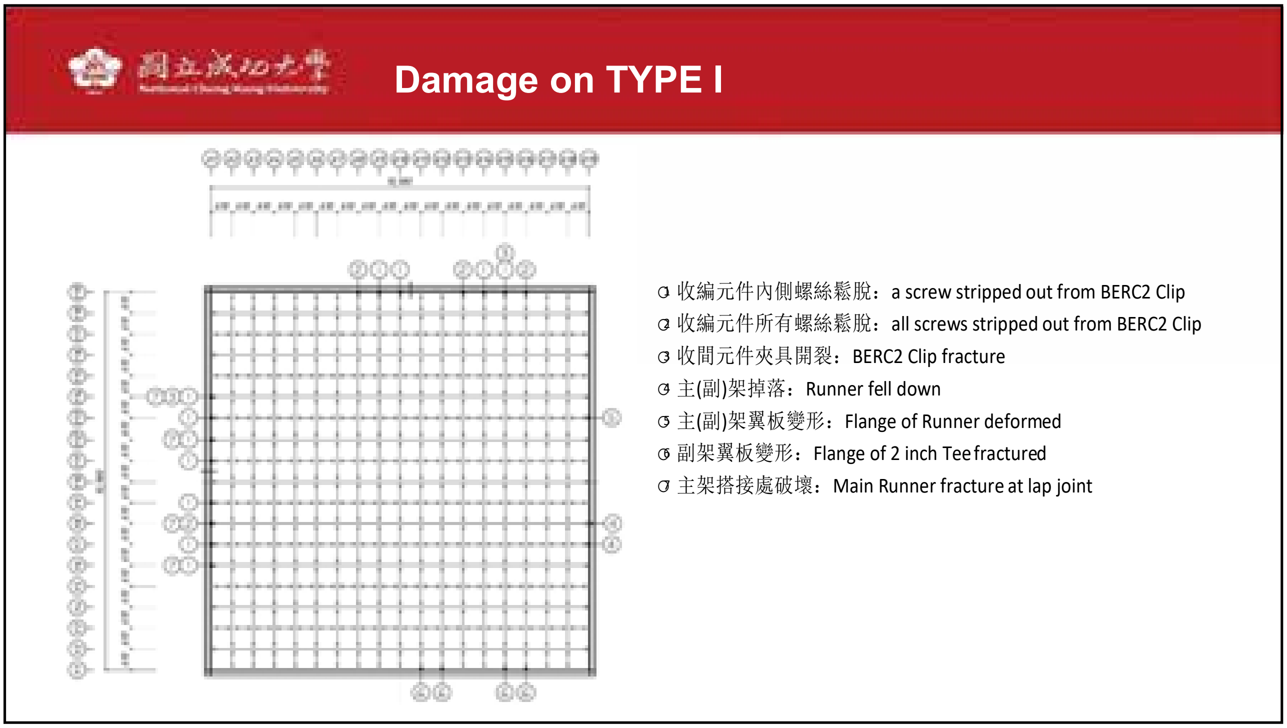

Damage on TYPE I

- 收編元件內側螺絲鬆脫：a screw stripped out from BERC2 Clip
- 收編元件所有螺絲鬆脫：all screws stripped out from BERC2 Clip
- 收間元件夾具開裂：BERC2 Clip fracture
- 主(副)架掉落：Runner fell down
- 主(副)架翼板變形：Flange of Runner deformed
- 副架翼板變形：Flange of 2 inch Tee fractured
- 主架搭接處破壞：Main Runner fracture at lap joint

Damage on TYPE II

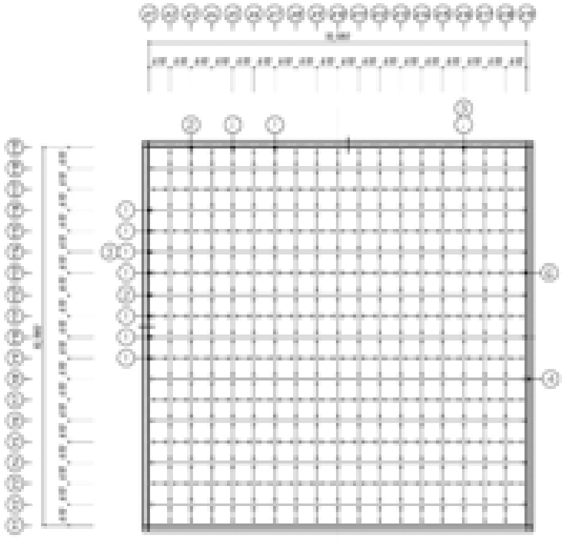

- 收編元件內側螺絲鬆脫：a screw stripped out from BERC2 Clip
- 收編元件所有螺絲鬆脫：all screws stripped out from BERC2 Clip
- 收間元件夾具開裂：BERC2 Clip fracture
- 主(副)架掉落：Runner fell down
- 主(副)架翼板變形：Flange of Runner deformed
- 副架翼板變形：Flange of 2 inch Tee fractured
- 主架搭接處破壞：Main Runner fracture at lap joint

Damage on TYPE III

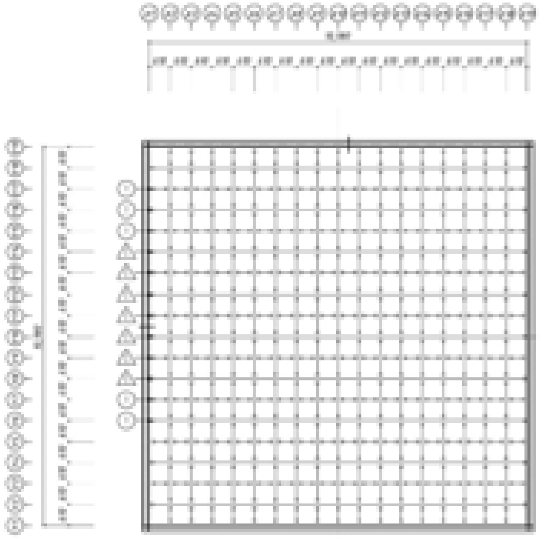

- 收編元件內側螺絲鬆脫：a screw stripped out from BERC2 Clip
- 收編元件所有螺絲鬆脫：all screws stripped out from BERC2 Clip
- 收間元件夾具開裂：BERC2 Clip fracture
- 主(副)架掉落：Runner fell down
- 主(副)架翼板變形：Flange of Runner deformed
- 副架翼板變形：Flange of 2 inch Tee fractured
- 主架搭接處破壞：Main Runner fracture at lap joint

Preliminary Findings (2019)

- All tested ceiling can endure the largest design PGA in Taiwan w/o falling objects.
- Bracing forces are still small.
- To be investigated
  - Low freq. excitation
  - Larger mass

SSB Background

- **SSB Damage in EQ**
  - Reduce the smoke control capacity in Fire Following EQ
  - Falling hazard

Basic Dynamic Behavior

Field ambient test to find f_n

- Length dependent

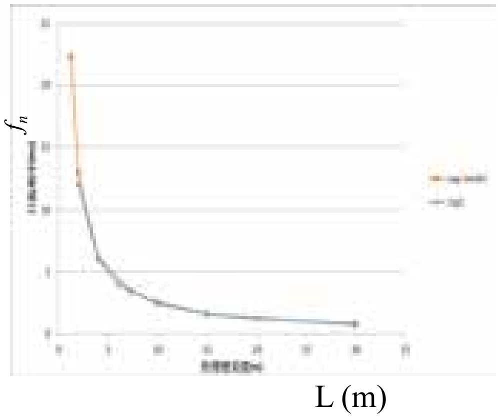

SAP2000 model established and verified by test model.

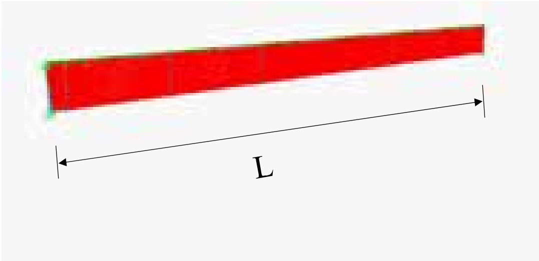

Shaking Table Test for SSB (2015)

Out-of-plane seismic performance

- ceiling + glass-type SSB
- AC 156
- PA of 300, 600, 800, 1000 gal
- @NCREE.

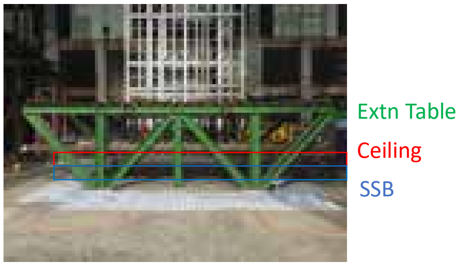

Results:

- Specimens easily cracked at End Panel or adjacent panel.

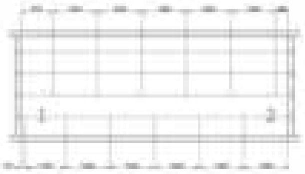

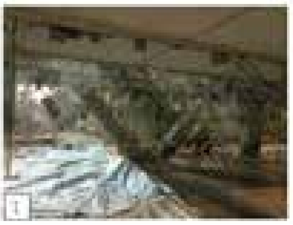

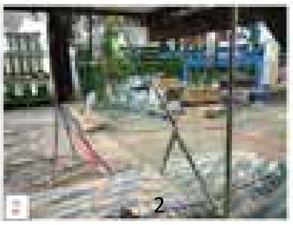

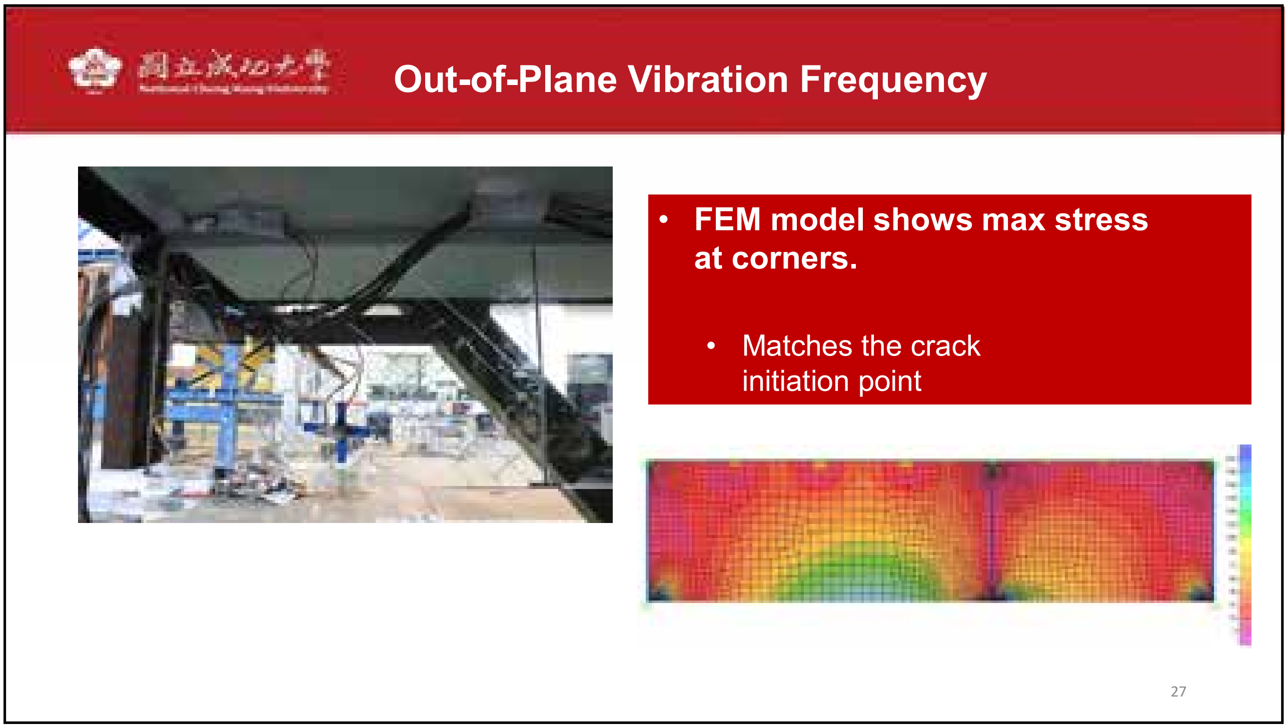

Out-of-Plane Vibration Frequency

- **FEM model shows max stress at corners.**
  - Matches the crack initiation point

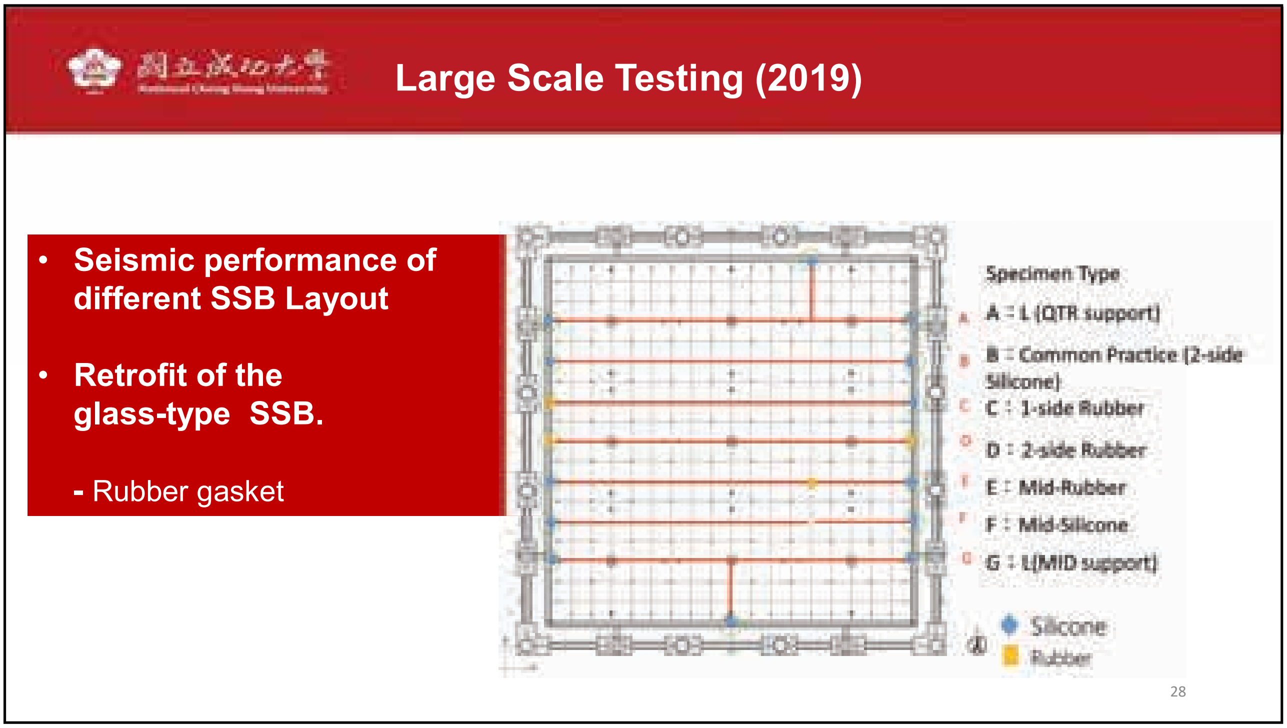

Large Scale Testing (2019)

- **Seismic performance of different SSB Layout**
- **Retrofit of the glass-type SSB.**

- Rubber gasket

Specimen Type
A : L (QTR support)
B : Common Practice (2-side Silicone)
C : 1-side Rubber
D : 2-side Rubber
E : Mid-Rubber
F : Mid-Silicone
G : L(MID support)

◆ Silicone
■ Rubber

Damage Patterns and PA

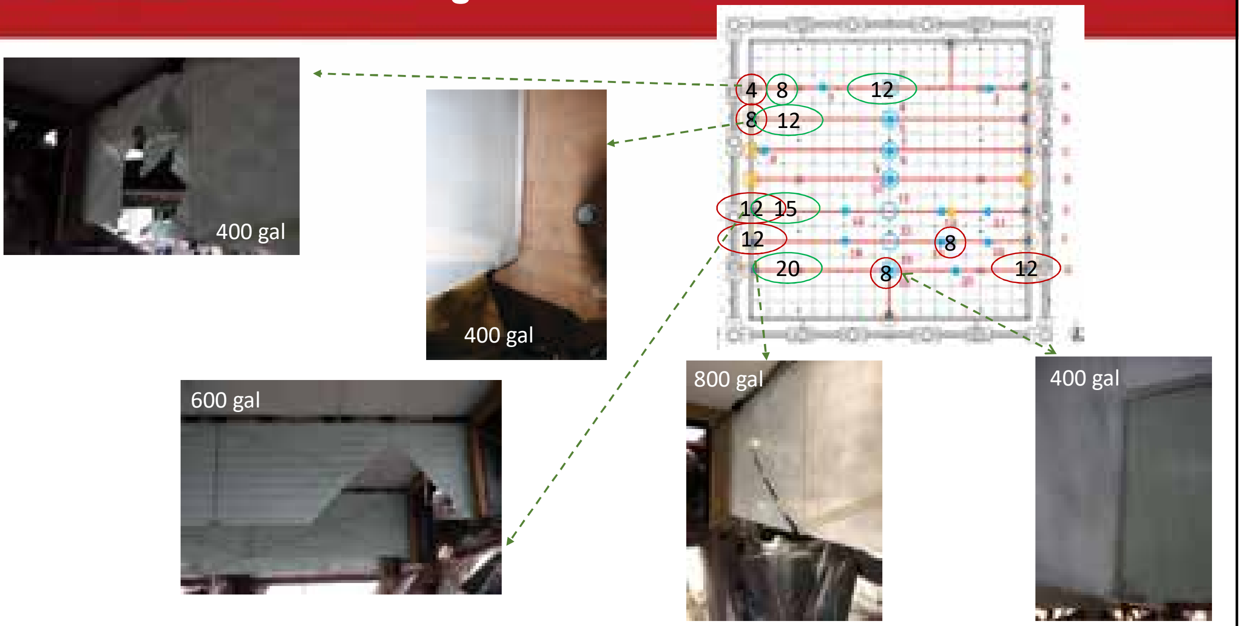
400 gal
400 gal
600 gal
800 gal
400 gal
4
8
12
8
12
12
15
12
8
20
8
12

Video of SSB testing

(AC 156)

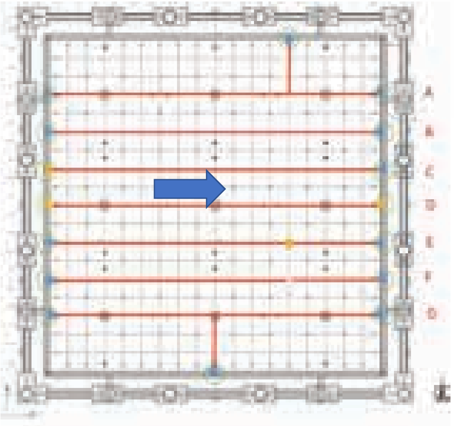

Findings from the Large Scale Testing

- **Damage of SSB at different excitation levels**
  - 40%(PA~400gal) (A-T type)Glass Crack Damage
  - 60%(PA~600gal) (B-Both ends use silicone)Serious Glass Crack
- **Retrofitted SSB performed well up to 800 gal.**

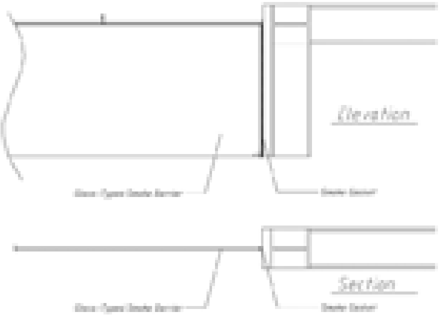

Acknowledgement:
Support from MOST and NCREE is important to these research projects.
My graduate students at NCKU.

Joint NRC-MOST Workshop-Earthquake Engineering Technologies 2019/10/08

Thank you for your attention!

STRUCTURAL HEALTH MONITORING OF APARTMENT COMPLEX BY MULTI-SCALE CROSS-SAMPLE ENTROPY: AN INFORMATION FLOW PERSPECTIVE

By Dr. T. K. Lin, National Chiao Tung University/ National Center for Research on Earthquake Engineering

Abstract

The aim of this study was to develop an entropy-based structural health monitoring system for solving the problem of unstable entropy values observed when multi-scale cross-sample entropy (MSCE) is employed to assess damage in real structures. Composite MSCE was utilized to enhance the reliability of entropy values on every scale. Additionally, the first mode of a structure was extracted using ensemble empirical mode decomposition to conduct entropy analysis and evaluate the accuracy of damage assessment. A seven-story model was created to validate the efficiency of the proposed method and the damage index. Subsequently, an experiment was conducted on a seven-story steel benchmark structure including 15 damaged cases to compare the numerical and experimental models. A confusion matrix was applied to classify the results and evaluate the performance over three indices: accuracy, precision, and recall. The results revealed the feasibility of the modified structural health monitoring system and demonstrated its potential in the field of long-term monitoring.

Keywords: multi-scale, cross-sample entropy, structural health monitoring.

Biography

Dr. Tzu-Kang Lin received his Ph.D. degree in Civil Engineering at National Taiwan University (2002). He was a visiting scholar of Stanford University (2007) which ignites his research in structural health monitoring. Currently, he is a Professor at National Chiao Tung University and the Adjunct Research Fellow of National Center for Research on Earthquake Engineering. His research interests include structural health monitoring, bio-inspired concept, and earthquake early warning, and bridge engineering.

NRC-MOST/NCREE Taiwan Workshop Earthquake Engineering Technologies
NRC Ottawa, Canada, October 7-9, 2019

Structural health monitoring of apartment complex by multi-scale cross-sample entropy: an information flow perspective

Tzu Kang Lin

National Chiao Tung University

Hsinchu, Taiwan

Outline

- ***Introduction***
- ***Methodology***
- ***Numerical Simulation***
- ***Analysis Results***
- ***Summary and Conclusion***

What's SHM

- *The process of implementing a damage detection strategy for aerospace, civil and mechanical engineering infrastructure is referred to as Structural Health Monitoring (SHM).*

- *The SHM process involves*
- *1. periodically sampled dynamic response measurements*
- *2. the extraction of damage-sensitive features*
- *3. the statistical analysis of features to determine the system health.*

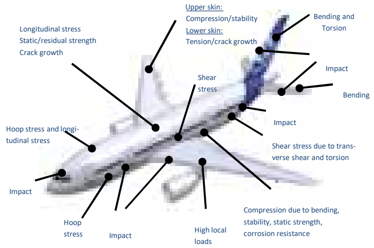
Upper skin:
Compression/stability
Lower skin:
Tension/crack growth
Bending and Torsion
Longitudinal stress
Static/residual strength
Crack growth
Impact
Shear stress
Bending
Hoop stress and longitudinal stress
Impact
Shear stress due to transverse shear and torsion
Impact
Compression due to bending, stability, static strength, corrosion resistance
Hoop stress
Impact
High local loads

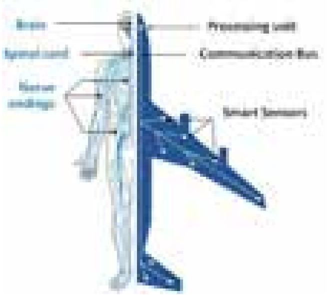
Brain
Spinal cord
Nerve endings
Processing unit
Communication Bus
Smart Sensors

Entropy

- *In thermodynamics, entropy is a measure of the number of specific ways, commonly understood as a measure of disorder.*

- *In information theory, entropy (more specifically, Shannon entropy) is the expected value(average) of the information contained in each message received.*

- *Messages don't have to be text; a message is simply any flow of information.*

- *The entropy of the message is its amount of uncertainty; it increases when the message is closer to random, and decreases when it is less random.*

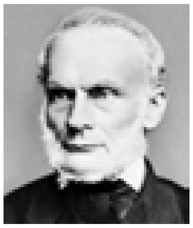

Rudolf Clausius (1822–1888)

Claude Elwood Shannon (1916–2001)

Information Flow

Nichols J M Examining structural dynamics using information flow *Probabilistic Eng. Mech.* 21 420–33 (2006)

- *Information flow in an information theoretical context is the transfer of information from a variable x to a variable y in a given process.*

- *Transfer entropy: a non-parametric statistic measuring the amount of directed (time-asymmetric) transfer of information between two random processes.*

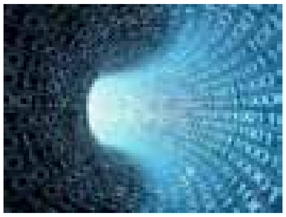

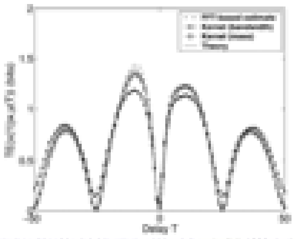

Damage Location Detection

Multi-scale Cross-Sample Entropy

Damage Index

- *Introduction*
- *Methodology*
- *Numerical Simulation*
- *Analysis Results*
- *Summary and Conclusion*

The proposed SHM concept

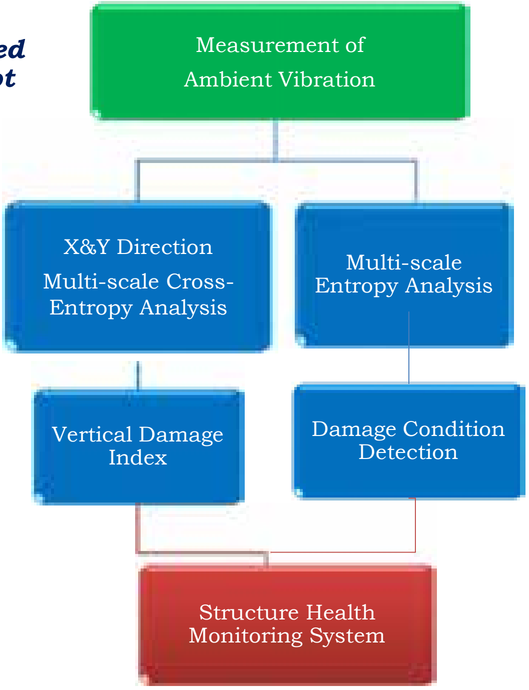
Measurement of Ambient Vibration

X&Y Direction Multi-scale Cross-Entropy Analysis

Multi-scale Entropy Analysis

Vertical Damage Index

Damage Condition Detection

Structure Health Monitoring System

SampEn

- **For a time series $\{X_i\} = \{x_1, \ldots, x_i, \ldots, x_N\}$ with length *N*, a vector $u_m(i) = \{x_i, x_{i+1}, \ldots, x_{i+m-1}\}$, $1 \le i \le N - m + 1$ of length *m* can be defined as the template.**

- **Various *N*-*m*+1 templates may compose the time series.**

- **The combination of all *N*-*m*+1 templates is represented by the template space *T*.**

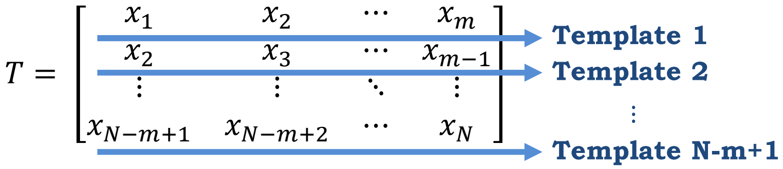

$$T = \begin{bmatrix} x_1 & x_2 & \cdots & x_m \\ x_2 & x_3 & \cdots & x_{m-1} \\ \vdots & \vdots & \ddots & \vdots \\ x_{N-m+1} & x_{N-m+2} & \cdots & x_N \end{bmatrix}$$

Template 1
Template 2
⋮
Template N-m+1

Number of similarities

- **The maximum distance d_{ij} between two templates $u_m(i)$ and $u_m(j)$ is expressed as**

$$d_{ij} = max\{|x(i + k) - x(j + k)| : 0 \le k \le m - 1\}$$

- **Next, the number of similarities $n_i^m(r)$ between the templates is calculated as**

$$n_i^m(r) = \sum_{j=1}^{N-m} d[u_m(i), u_m(j)]$$

- **where similarity is defined as**

$$d[u_m(i), u_m(j)] = \begin{cases} 1 & d_{ij} \le r \\ 0 & d_{ij} > r \end{cases}$$

Average Degree of Sample Similarity

- The degree of sample similarity $U_i^m(r)$ can then be calculated as

$$U_i^m(r) = \frac{n_i^m(r)}{(N - m - 1)}$$

- Next, the average degree of sample similarity $U^m(r)$ is expressed as

$$U^m(r) = \frac{1}{(N - m)} \sum_{i=1}^{N-m} U_i^m(r)$$

SampEn

- Subsequently, a new template space is created by assembling templates with length m+1.

- The procedure is repeated to calculate the average degree of sample similarity $U^{m+1}(r)$ of the new template space.

- Then, the SampEn value of the time series with parameters m, r, and N can be obtained as

$$S_E(m, r, N) = -\ln \frac{U^{m+1}(r)}{U^m(r)}$$

Coarse-graining Procedure

- **To construct multiple time series at different time scales, a time series undergoes a coarse-graining procedure.**

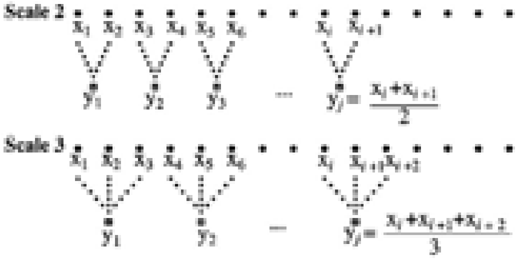
Scale 2
x_1 x_2 x_3 x_4 x_5 x_6 x_i x_{i+1}
y_1 y_2 y_3 ...
$y_j = \frac{x_i + x_{i+1}}{2}$
Scale 3
x_1 x_2 x_3 x_4 x_5 x_6 x_i x_{i+1} x_{i+2}
y_1 y_2 ...
$y_j = \frac{x_i + x_{i+1} + x_{i+2}}{3}$

- **SampEn is conducted for every coarse-grained time series $\left\{y_j^{(\tau)}\right\}$. This is defined as Multi-scale Entropy (MSE) analysis.**

Multi-scale Cross-sample Entropy

- **The two original signals undergo the coarse-graining procedure, and Cross-SampEn is conducted on the new time series. This is defined as Multi-scale Cross-Sample Entropy (MSCE).**
- **The Cross-SampEn values obtained are plotted as a function of the scale factor τ $(f(\tau) = CS_E)$.**

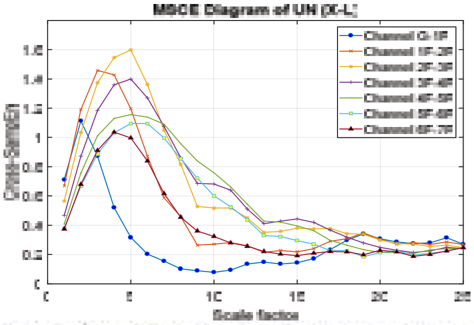

Damage Index

- **If the DI is positive, then the floor is classified as damaged. A negative DI denotes that the floor is undamaged.**

Undamaged

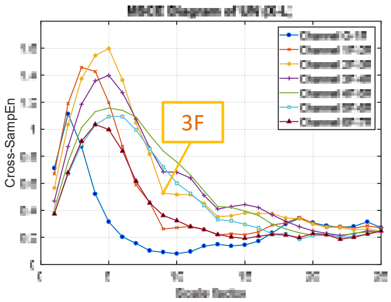

Damage on third floor

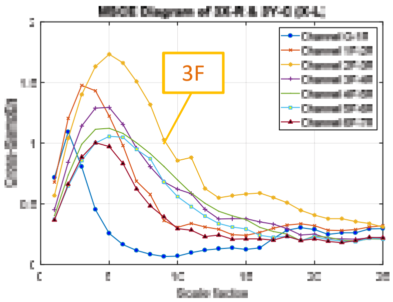

- *Introduction*
- *Methodology*
- *Numerical Simulation*
- *Analysis Results*
- *Summary and Conclusion*

The Numerical Model

- Steel, 7-story model.
- Three bays on the x-axis, single bay on the y-axis
- Story height: 1.06m
- X-axis bay width: 1.32m
- Y-axis bay width: 0.92m
- Columns: 75x50mm steel plates
- Beams: 70x100mm steel plates
- Bracing: 65x65x6mm L-shaped steel angles

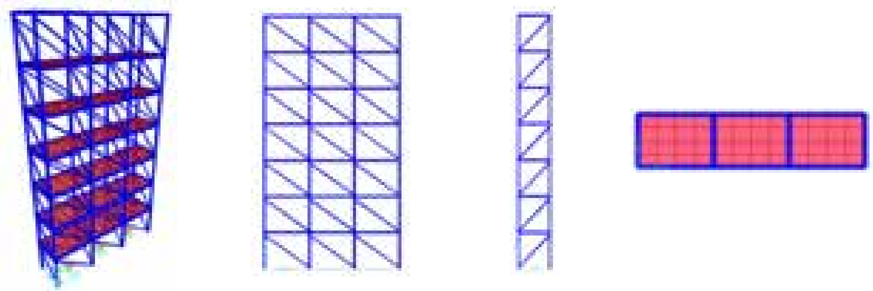

3D view, front and back view, side view, and top view of the model

---

Damage Database

- **Modal and time history analyses are performed on the model in SAP2000.**
- **The input ground acceleration in the x- and y-axes is the white noise signal.**
- **The output is of 30,000 points sampled at 200 Hz.**

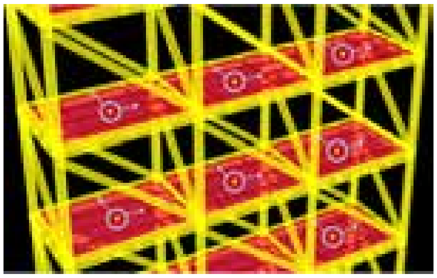

The biaxial velocity response data is extracted per bay from the center of each floor.

Damage Database (cont'd)

The damage cases consist of various combinations of single-story, two-story or multistory damage, paired with single- or multi-bay, and single- or multi-direction damage.

Case Number	Damage Group	Damaged Floor, Direction and Bay
19	Multistory, single-bay, single-direction	3X-L & 4X-L & 6X-L
20		1Y-R & 4Y-R & 7Y-R
21	Multistory, single-bay, multidirectional	4X-L & 5Y-L & 6Y-L
22		1XY-C & 3XY-C & 5XY-C
✦ 23	Multistory, multi-bay, single-direction	3X-L & 4X-C & 5X-R
24		6Y-L & 2Y-C & 7Y-R
25	Multistory, multi-bay, multidirectional	1X-R & 2X-R & 1Y-L
✦ 26		7XY-R & 4Y-L & 6Y-C

- *Introduction*
- *Methodology*
- *Numerical Simulation*
- *Analysis Results*
- *Summary and Conclusion*

MSCE Analysis

- **The velocity signals for the X- and Y-axes were extracted from the center of each floor.**
- **The signals of two vertically adjacent floors under the same damage condition were processed by MSCE to evaluate the dissimilarity between floors.**

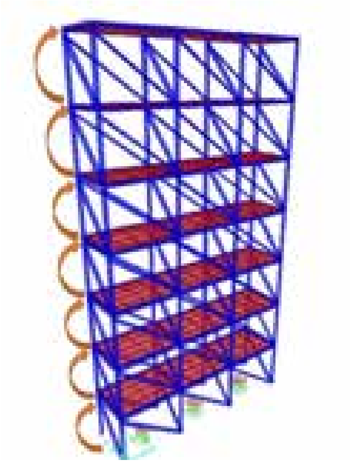

MSCE Analysis Results

UN (X-L)

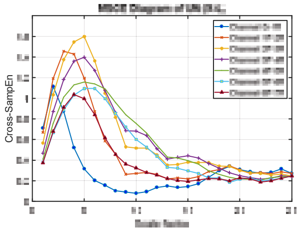

UN (X-C)

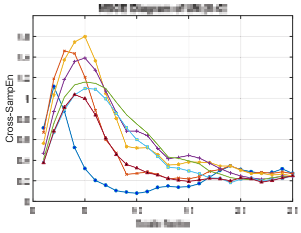

UN (X-R)

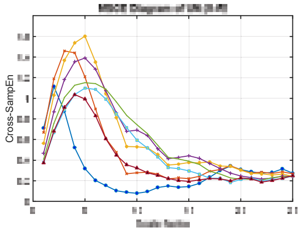

UN (Y-L)

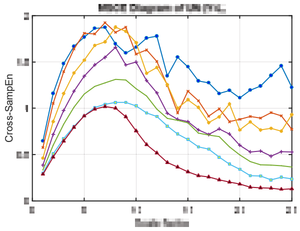

UN (Y-C)

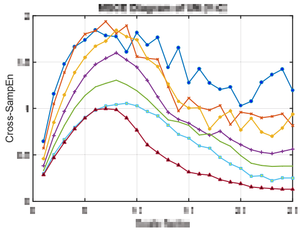

UN (Y-R)

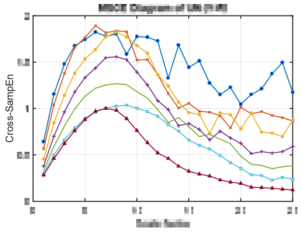

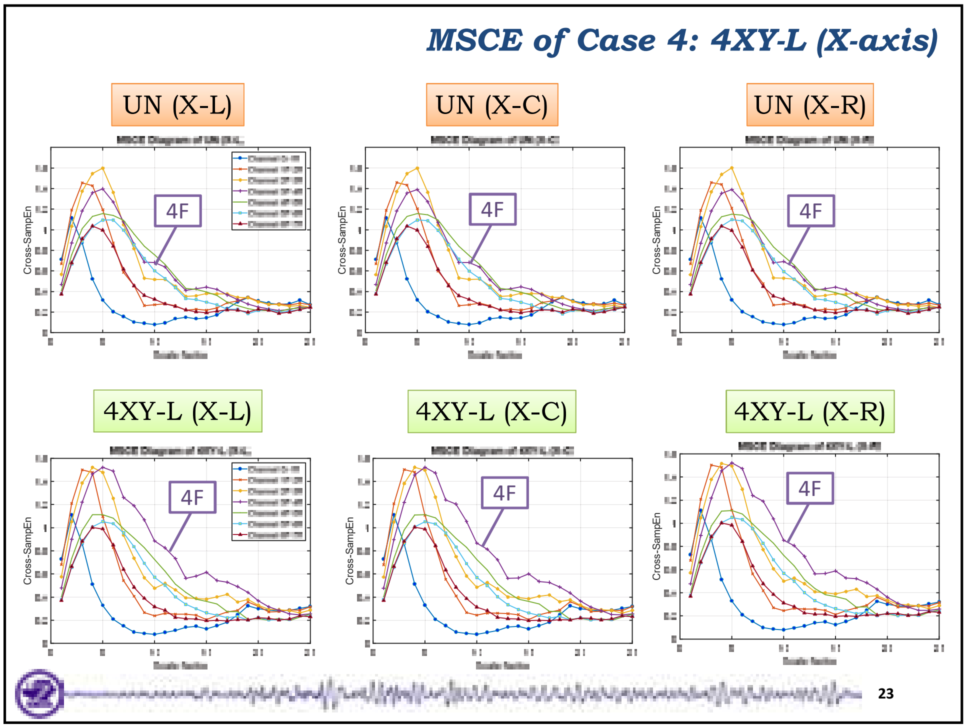

MSCE of Case 4: 4XY-L (X-axis)

UN (X-L)

UN (X-C)

UN (X-R)

4XY-L (X-L)

4XY-L (X-C)

4XY-L (X-R)

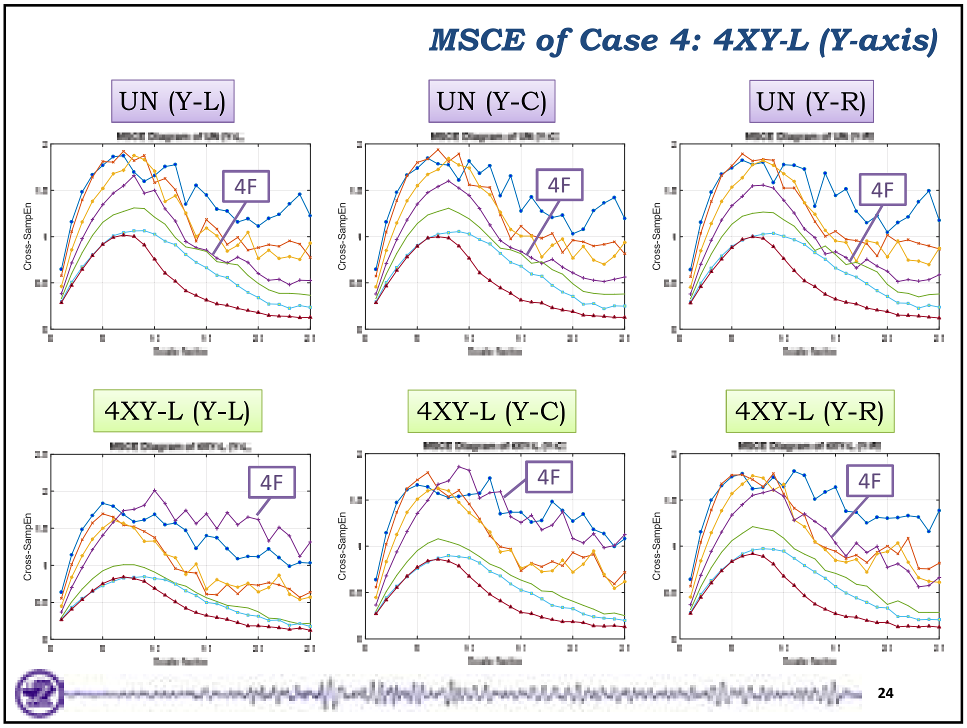

MSCE of Case 4: 4XY-L (Y-axis)

UN (Y-L)

UN (Y-C)

UN (Y-R)

4XY-L (Y-L)

4XY-L (Y-C)

4XY-L (Y-R)

DI of Case 4: 4XY-L

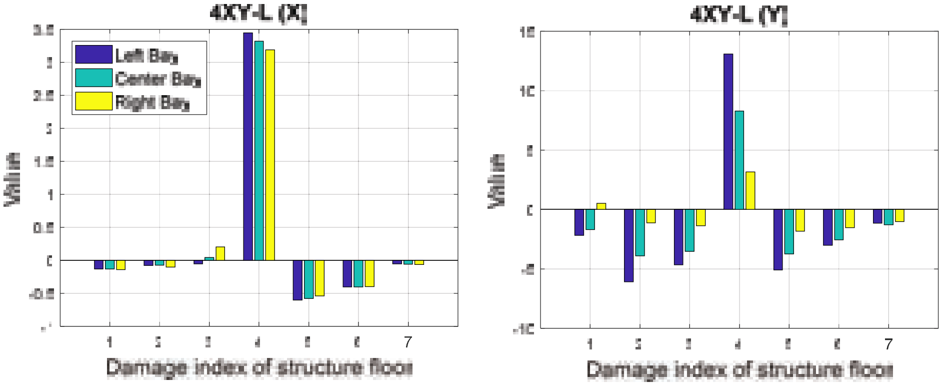

DI of Case 4: 4XY-L

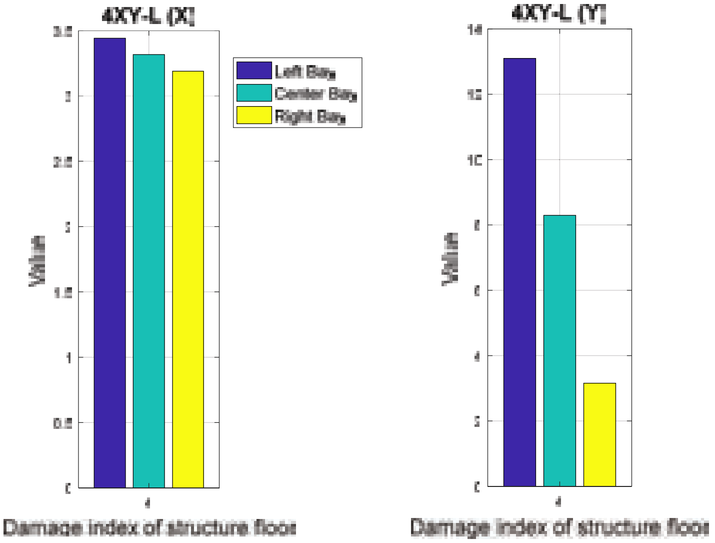

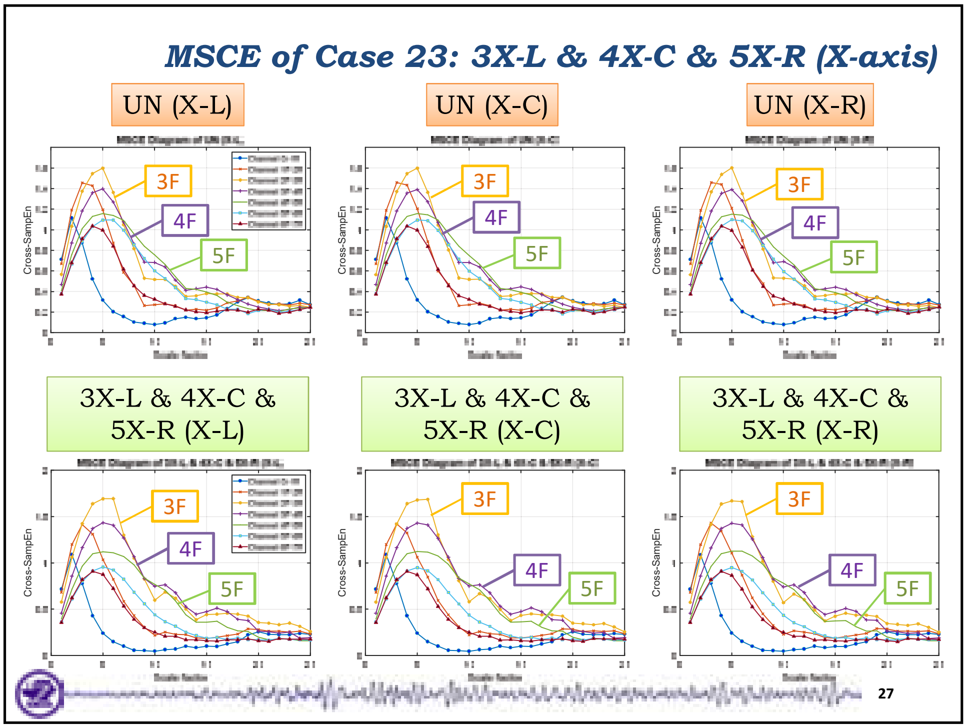

MSCE of Case 23: 3X-L & 4X-C & 5X-R (X-axis)

UN (X-L)

UN (X-C)

UN (X-R)

3X-L & 4X-C & 5X-R (X-L)

3X-L & 4X-C & 5X-R (X-C)

3X-L & 4X-C & 5X-R (X-R)

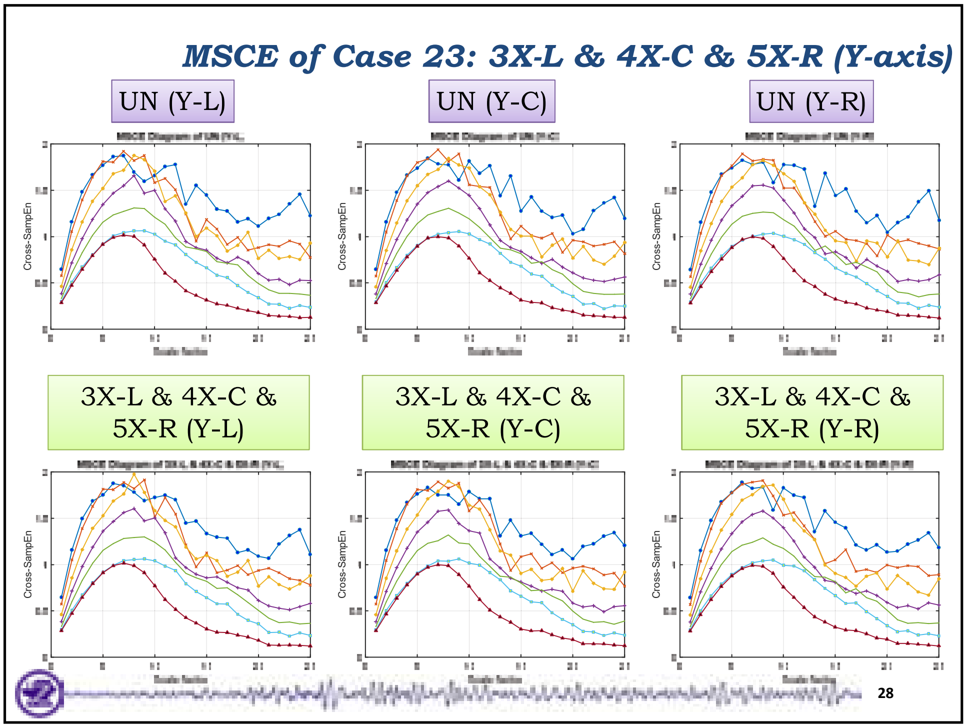

MSCE of Case 23: 3X-L & 4X-C & 5X-R (Y-axis)

UN (Y-L)

UN (Y-C)

UN (Y-R)

3X-L & 4X-C & 5X-R (Y-L)

3X-L & 4X-C & 5X-R (Y-C)

3X-L & 4X-C & 5X-R (Y-R)

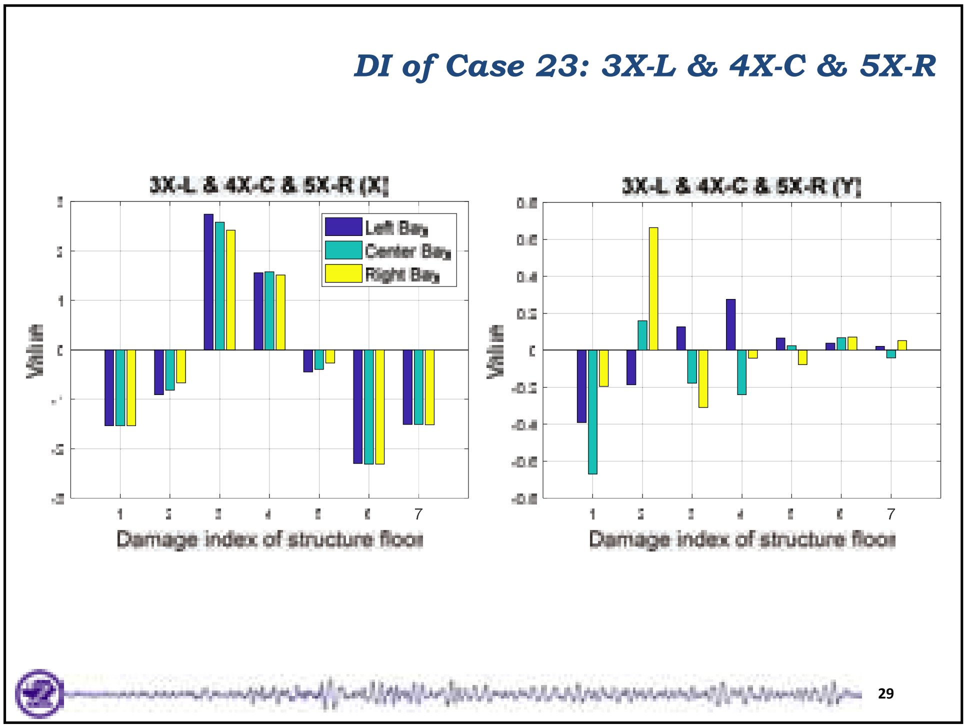

DI of Case 23: 3X-L & 4X-C & 5X-R

29

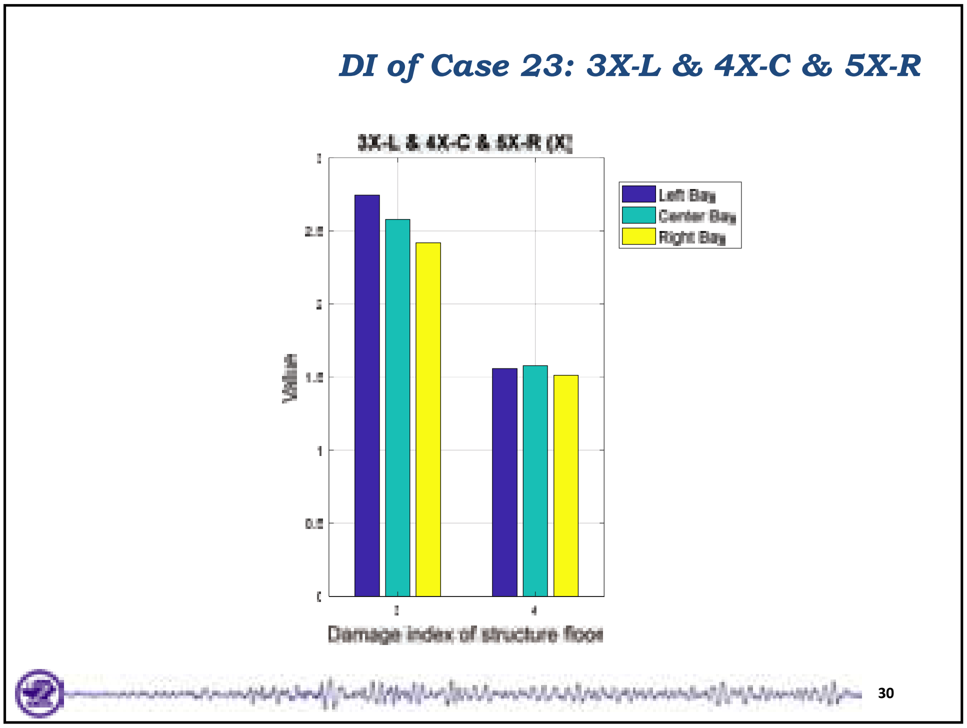

DI of Case 23: 3X-L & 4X-C & 5X-R

30

Damaged Floors and Directions Classification Results

- **The DI results are classified into four categories:**
  - **True Positives (TP)**
  - **False Positives (FP)**
  - **True Negatives (TN)**
  - **False Negatives (FN)**
- **Precision and recall are calculated as:**

$$\text{Precision} = \frac{\text{TP}}{\text{TP} + \text{FP}}$$

$$\text{Recall} = \frac{\text{TP}}{\text{TP} + \text{FN}}$$

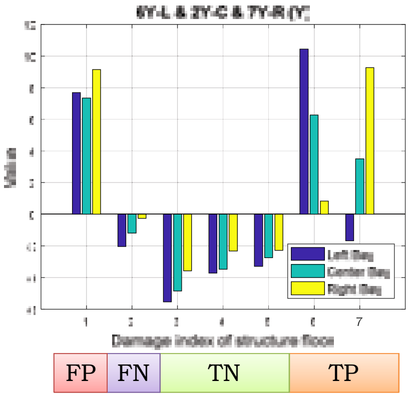

Damaged Floors and Directions Classification Results

Direction	True Positives	False Positives	True Negatives	False Negatives
X	25	0	151	6
Precision = 100% Recall = 81%				

Direction	True Positives	False Positives	True Negatives	False Negatives
Y	30	11	139	2
Precision = 73% Recall = 94%				

The overall results for both axes yield a precision of 83% and a recall of 87% for the classification of damaged locations and directions.

Classification of Damaged Bays Results

- **The results for the classification of damaged bays were analyzed separately.**
- **Each damage instance indicates the symmetric removal of bracings.**

Direction	Damage Instances	Correctly Classified Bay	Accuracy
X	34	24	71%
Y	34	27	79%

- **The overall accuracy for classification of bays in both directions is of 75%.**

- ***Introduction***
- ***Methodology***
- ***Numerical Simulation***
- ***Analysis Results***
- ***Summary and Conclusions***

Summary and Conclusion

- The feasibility of detecting damage on an apartment complex by an SHM system comprised of the MSCE and DI methods was demonstrated.
- An overall precision of 83% and a recall of 87% were obtained for the classification results of the damaged floor and direction.
- An accuracy of 75% for the classification of damaged bays was obtained.
- The high potential of implementing the SHM system in large complex structures quickly and at low cost can be expected.

Thanks for your attention

MODELLING OF SEISMIC-DEFICIENT AND REPAIRED RC STRUCTURES: CHALLENGES AND INNOVATIVE SOLUTIONS

By Dr. V. Sadeghian, Carleton University

Abstract

The existing modelling methods for seismic performance assessment of reinforced concrete (RC) structures can be classified into two groups: micro models and macro models. Micro models are computationally expensive and limited to the component-level analysis, while macro models use simplifying assumptions in their formulations and cannot accurately capture the response of structures with highly nonlinear behaviour. In this study, a novel multi-platform modelling approach is presented which enables to integrate macro models with micro models to accurately analyze the response of structures at both the component-level and system-level. In this approach, each potentially critical member is modelled in a local finite element analysis tool, while the remainder of the system is modelled with a computationally fast global analysis software. The analysis procedure considers the interactions between different substructures by satisfying the equilibrium and compatibility conditions. The effectiveness of the proposed modelling method is verified by various case studies including quasi-static cyclic analysis of RC structures repaired with fibre-reinforced polymer wraps.

Keywords: reinforced concrete, nonlinear analysis, seismic behaviour, repaired structures, fibre-reinforced polymer.

Biography

Dr. Vahid Sadeghian is an Assistant Professor at Carleton University. Vahid received his B.Sc. degree from the University of Tehran, and his M.Sc. and Ph.D. degrees from the University of Toronto. Before joining Carleton University, he worked as a Structural Engineer at Arup in Toronto. His research focus is on the development of advanced analytical and experimental methods for performance and safety assessment of reinforced concrete structures.

MODELLING SEISMIC-DEFICIENT AND REPAIRED RC STRUCTURES

CHALLENGES AND INNOVATIVE SOLUTIONS

Vahid Sadeghian
Assistant Professor, PhD

Oct 2019

Modelling Methods for RC Structures

Macro-Models

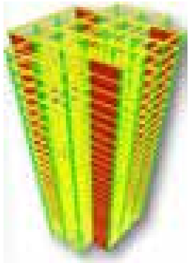

- ✓ Computationally fast
- ✗ Simplifying assumptions

System-level response

Micro-Models

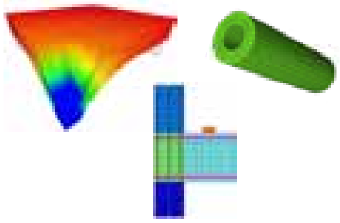

- ✗ Computationally expensive
- ✓ Better accuracy

Component-level response

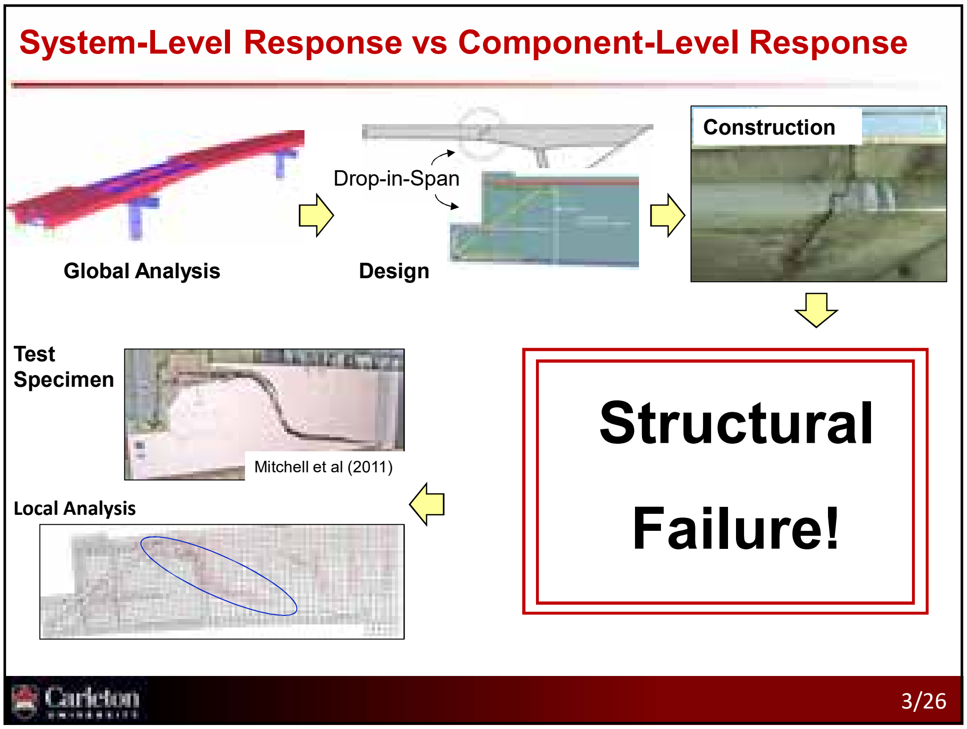

System-Level Response vs Component-Level Response

Global Analysis

Drop-in-Span

Design

Construction

Structural

Failure!

Test Specimen

Mitchell et al (2011)

Local Analysis

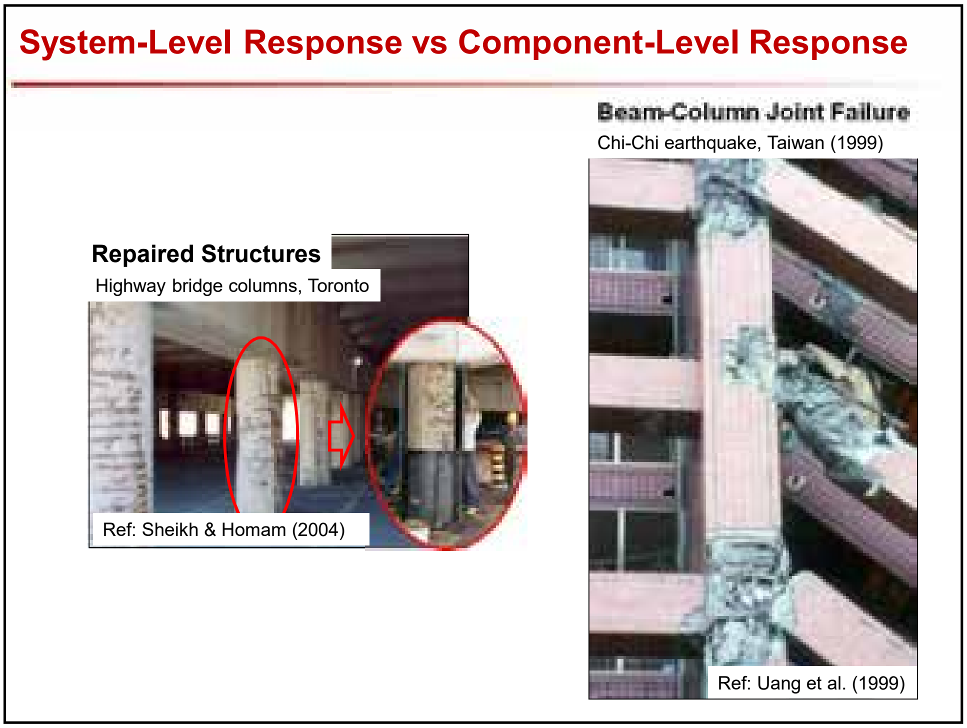

System-Level Response vs Component-Level Response

Repaired Structures

Highway bridge columns, Toronto

Ref: Sheikh & Homam (2004)

Beam-Column Joint Failure

Chi-Chi earthquake, Taiwan (1999)

Ref: Uang et al. (1999)

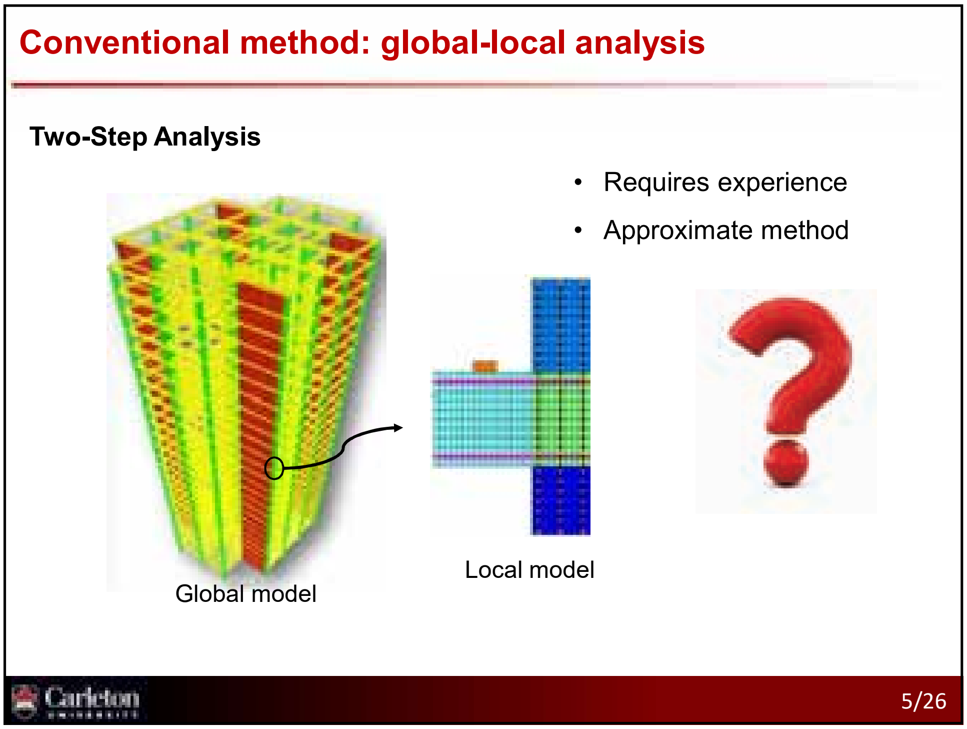

Conventional method: global-local analysis

Two-Step Analysis

- Requires experience
- Approximate method

Global model
Local model

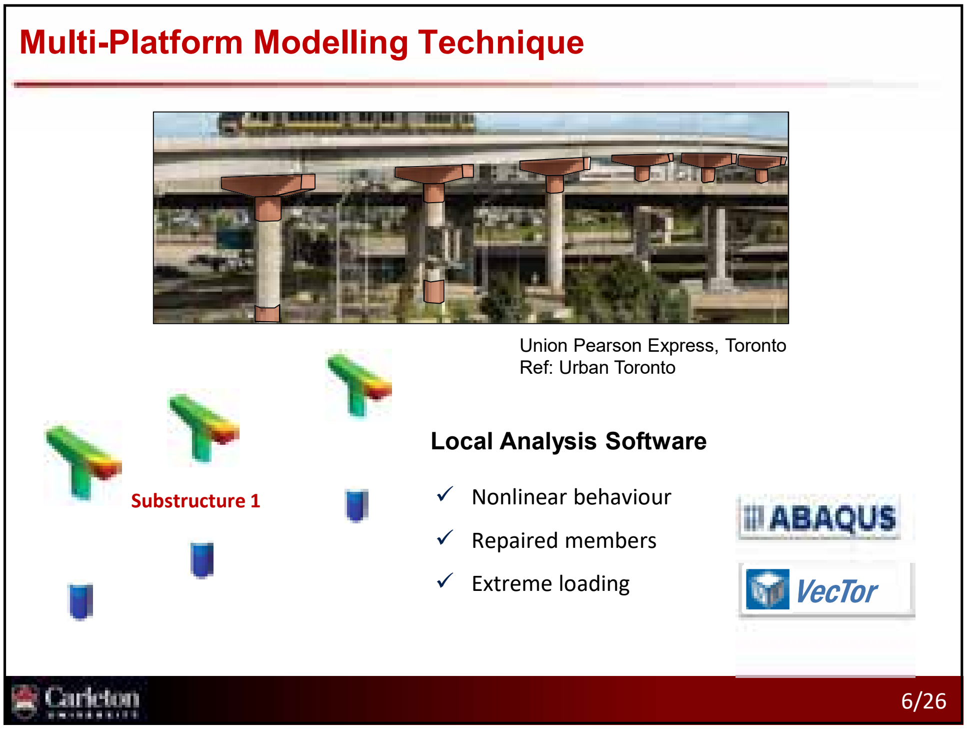

Multi-Platform Modelling Technique

Union Pearson Express, Toronto
Ref: Urban Toronto

Substructure 1

Local Analysis Software

- ✓ Nonlinear behaviour
- ✓ Repaired members
- ✓ Extreme loading

ABAQUS
VecTor

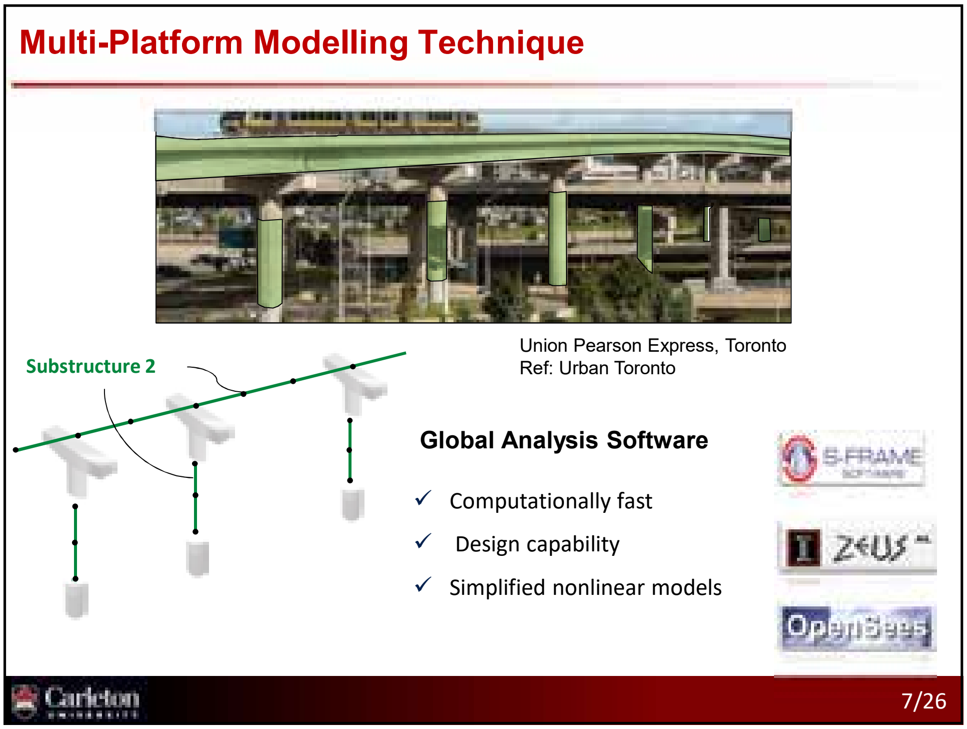

Multi-Platform Modelling Technique

Union Pearson Express, Toronto
Ref: Urban Toronto

Global Analysis Software

- ✓ Computationally fast
- ✓ Design capability
- ✓ Simplified nonlinear models

S-FRAME SOFTWARE

ZEUS

OpenSees

Carleton UNIVERSITY

7/26

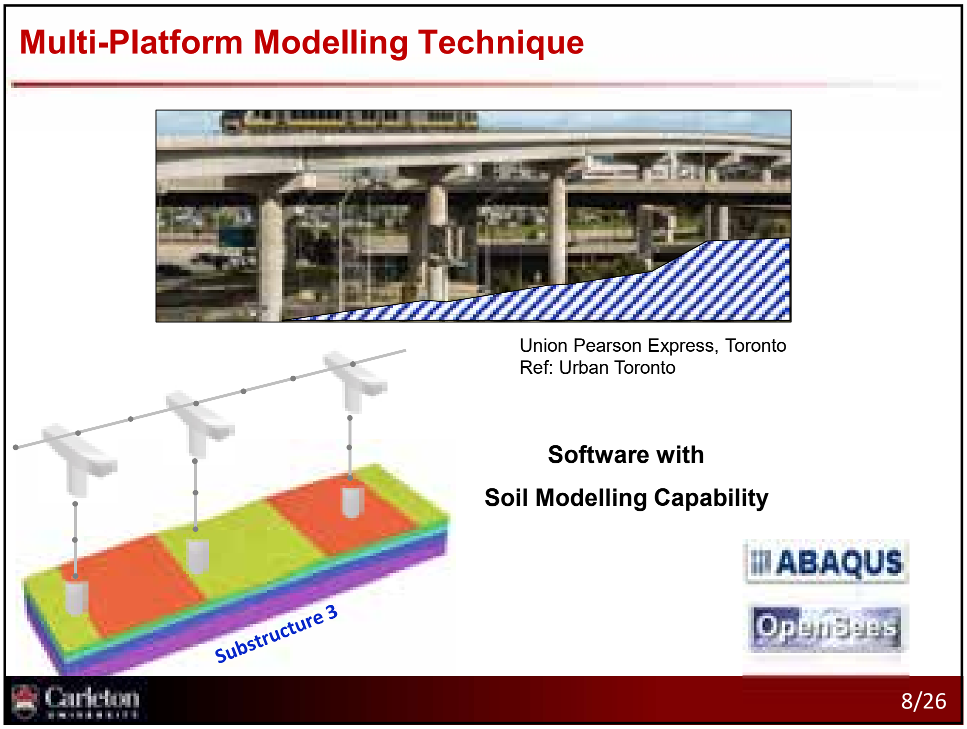

Multi-Platform Modelling Technique

Union Pearson Express, Toronto
Ref: Urban Toronto

Software with

Soil Modelling Capability

ABAQUS

OpenSees

Carleton UNIVERSITY

8/26

Multi-Platform Modelling Technique

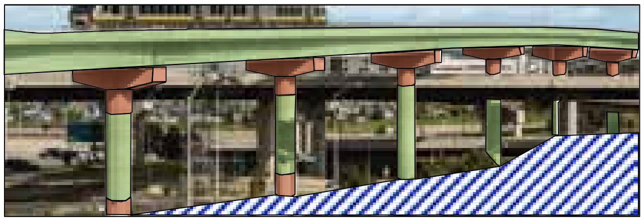

Union Pearson Express, Toronto
Ref: Urban Toronto

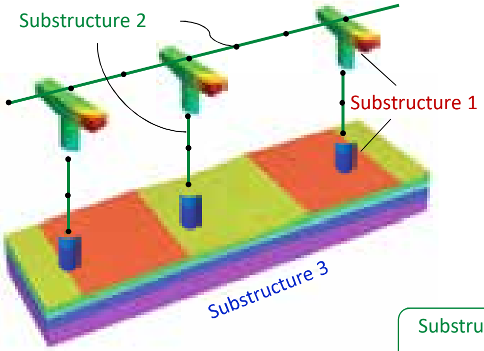
Substructure 2
Substructure 1
Substructure 3

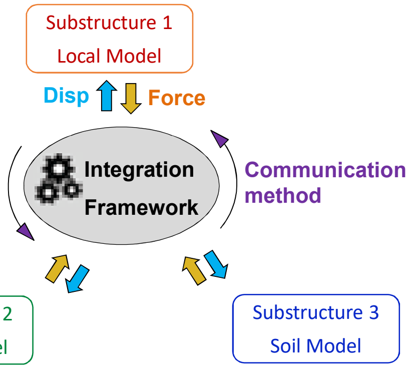
Substructure 1
Local Model
Disp
Force
Integration
Framework
Communication
method
Substructure 2
Global Model
Substructure 3
Soil Model

Cyrus Integration Framework

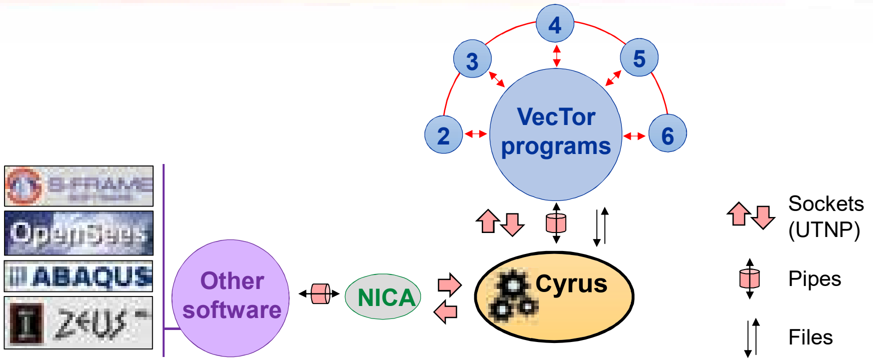
4
3
5
2
VecTor
programs
6
S-FRAME
OpenSees
ABAQUS
ZEUS
Other
software
NICA
Cyrus
Sockets
(UTNP)
Pipes
Files

UTNP Standardized Data Exchange Format

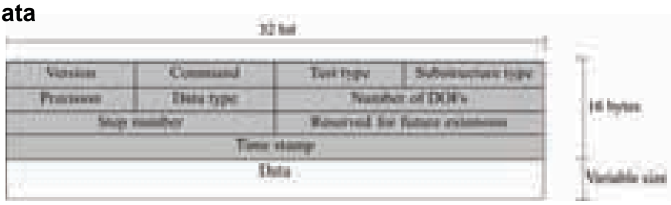
32 bit
16 bytes
Variable size

Version	Command	Test type	Substructure type
Precision	Data type	Number of DOFs	
Step number		Reserved for future extensions	
Time stamp			
Data			

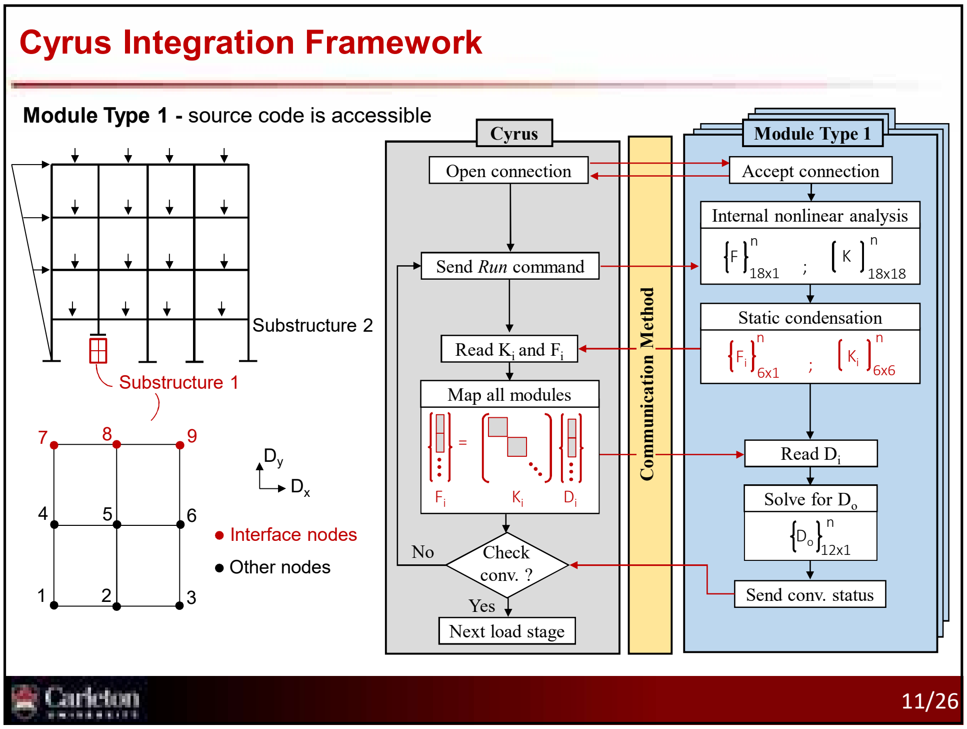

Cyrus Integration Framework

Module Type 1 - source code is accessible

Substructure 2
Substructure 1
7
8
9
4
5
6
1
2
3
D_y
D_x
● Interface nodes
● Other nodes
Cyrus
Open connection
Send *Run* command
Read K_i and F_i
Map all modules
F_i
K_i
D_i
No
Check conv. ?
Yes
Next load stage
Communication Method
Module Type 1
Accept connection
Internal nonlinear analysis
$\{F\}^n_{18x1}$; $[K]^n_{18x18}$
Static condensation
$\{F_i\}^n_{6x1}$; $[K_i]^n_{6x6}$
Read D_i
Solve for D_o
$\{D_o\}^n_{12x1}$
Send conv. status
Carleton
11/26

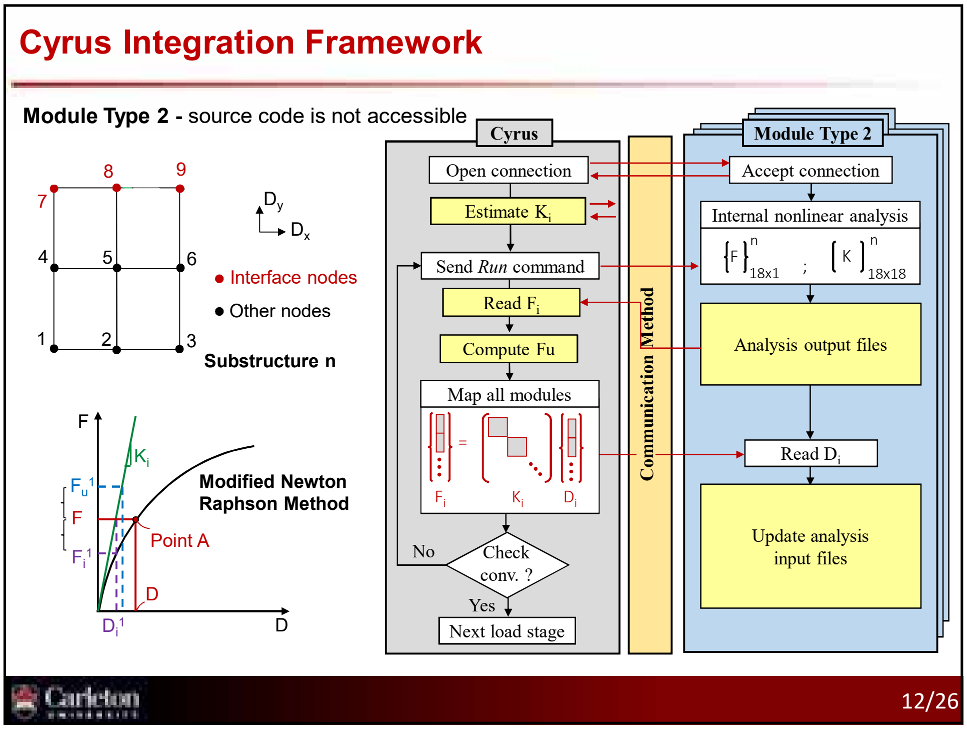

Cyrus Integration Framework

Module Type 2 - source code is not accessible

8
9
7
4
5
6
1
2
3
D_y
D_x
● Interface nodes
● Other nodes
Substructure n
F
K_i
F_u^1
F
F_i^1
Modified Newton Raphson Method
Point A
D
D_i^1
D
Cyrus
Open connection
Estimate K_i
Send *Run* command
Read F_i
Compute Fu
Map all modules
F_i
K_i
D_i
No
Check conv. ?
Yes
Next load stage
Communication Method
Module Type 2
Accept connection
Internal nonlinear analysis
$\{F\}^n_{18x1}$; $[K]^n_{18x18}$
Analysis output files
Read D_i
Update analysis input files
Carleton
12/26

Application Example 1: Older RC Frame (Calvi et al. 2002)

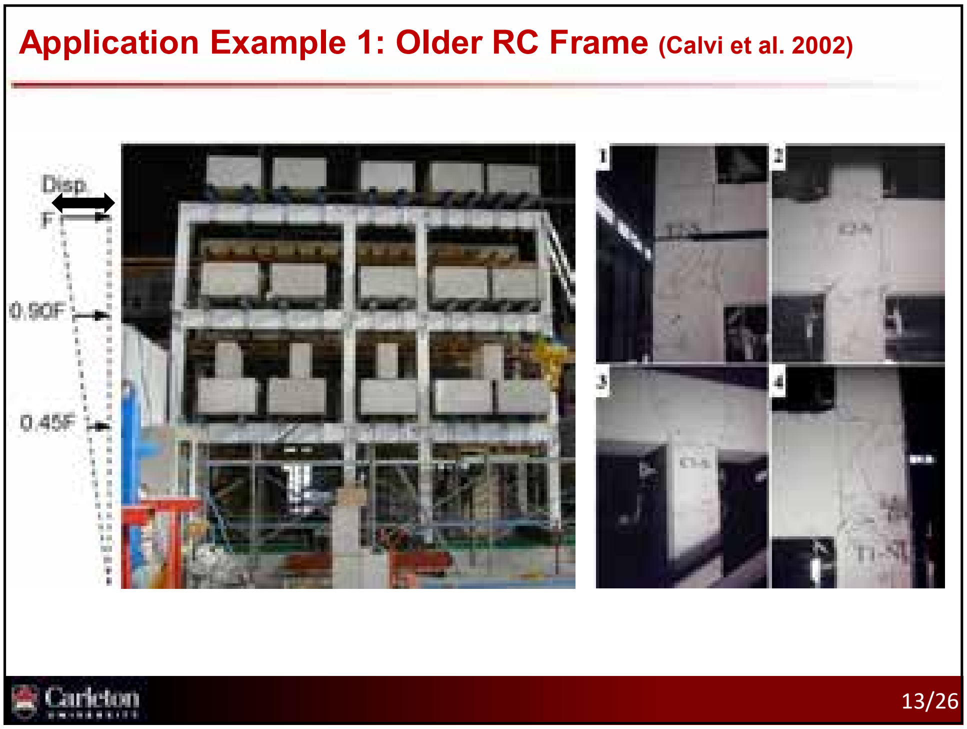
Disp.
F
0.90F
0.45F
1
2
3
4

Application Example 1: Older RC Frame (Calvi et al. 2002)

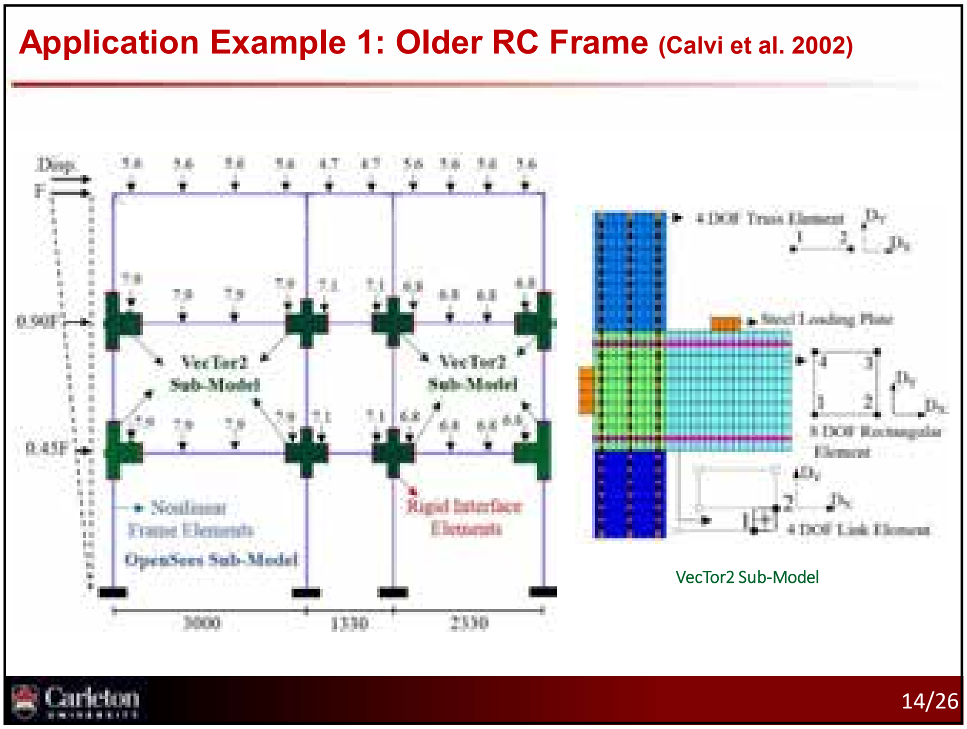
Disp.
F
0.90F
0.45F
5.6 5.6 5.6 5.6 4.7 4.7 5.6 5.6 5.6 5.6
7.9 7.9 7.9 7.9 7.1 7.1 6.8 6.8 6.8 6.8
VecTor2 Sub-Model
VecTor2 Sub-Model
Nonlinear Frame Elements
OpenSees Sub-Model
Rigid Interface Elements
3000
1330
2330
4 DOF Truss Element
Steel Loading Plate
8 DOF Rectangular Element
4 DOF Link Element
D_Y
D_X
1
2
3
4

VecTor2 Sub-Model

Application Example 1: Older RC Frame (Calvi et al. 2002)

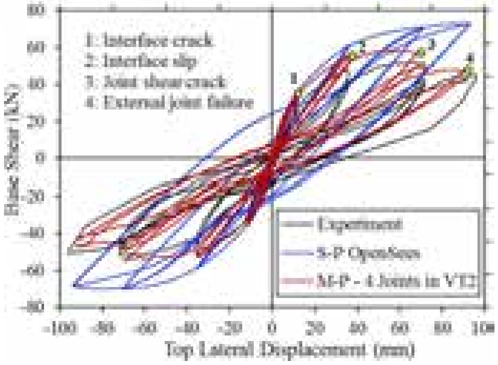

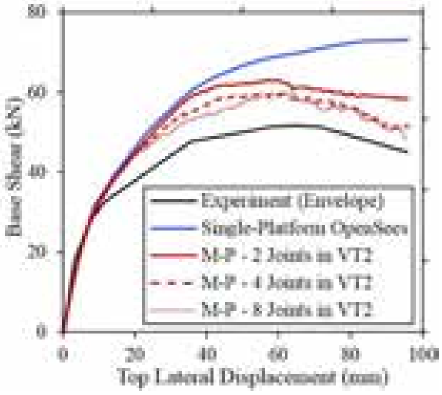

Application Example 1: Older RC Frame (Calvi et al. 2002)

Crack Patterns and Deflected Shape

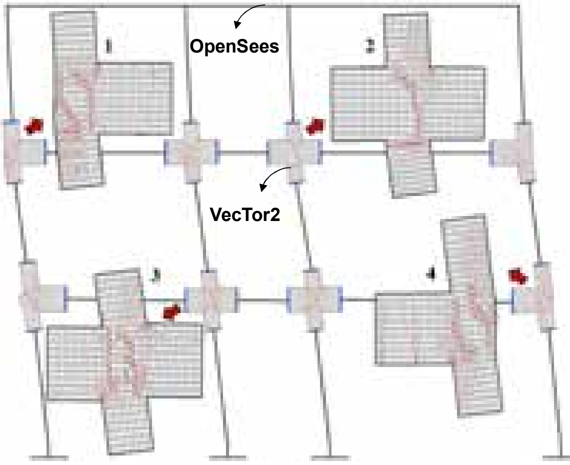
OpenSees
VecTor2
1
2
3
4

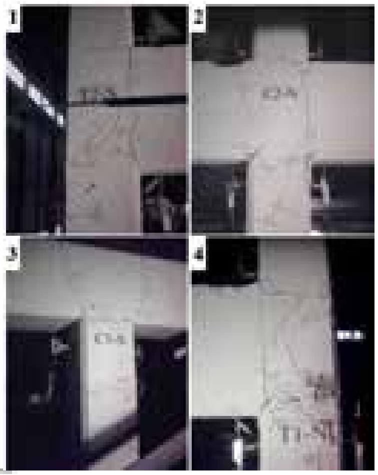
1
2
3
4
T2-S
T1-N

Modelling the Interface Between Sub-Models

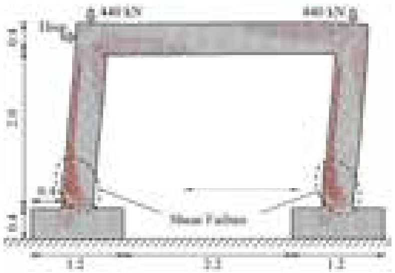

Disp.
440 kN
440 kN
0.4
2.6
0.4
0.4
Shear Failure
1.2
3.2
1.2

Single-Platform Model (VecTor2)

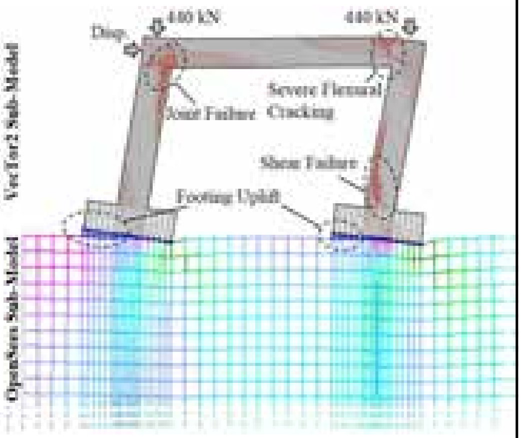

VecTor2 Sub-Model
OpenSees Sub-Model
Disp.
440 kN
440 kN
Joint Failure
Severe Flexural Cracking
Shear Failure
Footing Uplift

Multi-Platform Model (VecTor2 + OpenSees)

FRP-Repaired Structures: Component-Level Response

Memon & Sheikh, 2005

	Initial Damage	GFRP Layers	(P/P_o)
1	Cont.	None	0.56
2	No	2	0.33
3	No	4	0.56
4	No	2	0.56
5	No	1	0.33
6	No	6	0.56
7	Yes	2	0.33
8	Yes	6	0.56

FRP-Repaired Structures: Component-Level Response

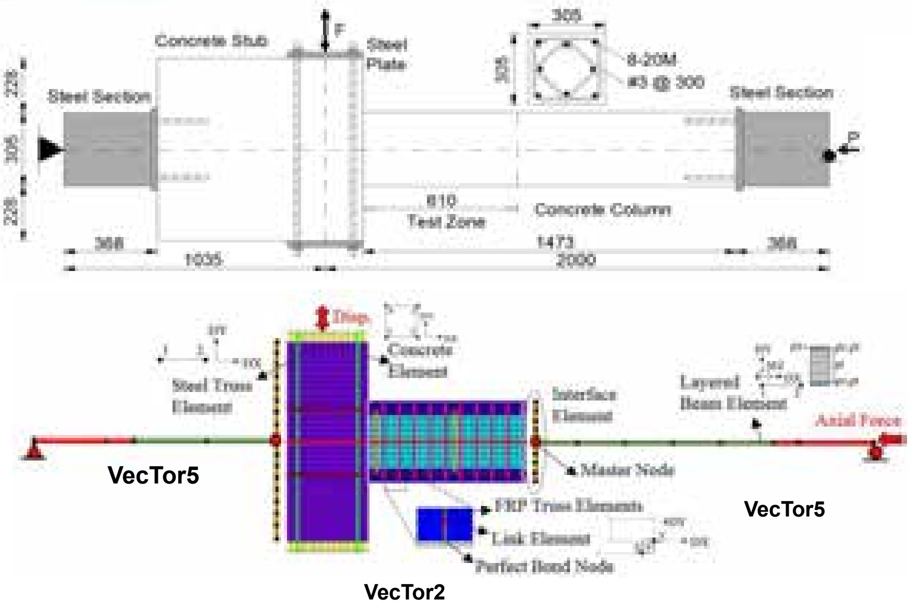
Concrete Stub
F
Steel Plate
305
305
8-20M
#3 @ 300
Steel Section
Steel Section
P
228
305
228
810
Test Zone
Concrete Column
368
1035
1473
2000
368
Disp.
Concrete Element
Steel Truss Element
Interface Element
Layered Beam Element
Axial Force
Master Node
FRP Truss Elements
Link Element
Perfect Bond Node
VecTor5
VecTor5
VecTor2

FRP-Repaired Structures: Component-Level Response

⟐ RC-Related Mechanisms

Reinforcement Buckling

Akkaya et al. (2013) model

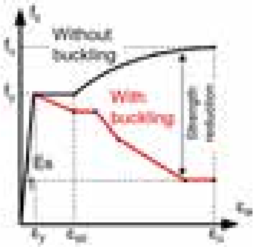

Concrete Cover Spalling

- $\varepsilon_{c2} < -3.5 \times 10^{-3}$
- $W_c < 2.0$ mm

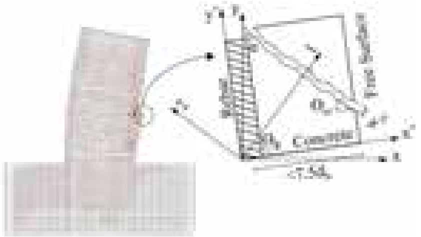
Free Surface
Concrete

Damage History

Initial Analysis

Record Damage (Binary File)

Repaired Analysis

FRP-Repaired Structures: Component-Level Response

◈ **FRP-Related Mechanisms**

Bond-Slip Effects

Nakaba model (2001)

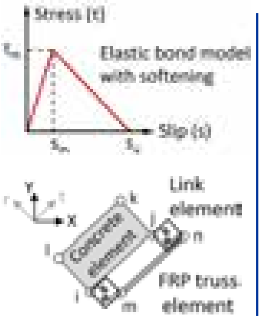
Stress (τ)
$τ_m$
Elastic bond model with softening
Slip (s)
s_m
s_u
Y
X
k
Link element
l
n
Concrete element
FRP truss element
m

Confinement Effects

Smeared out-of-plane
FRP Component

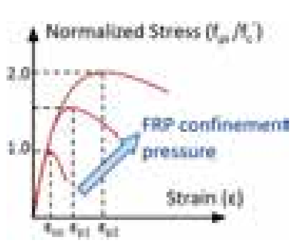

Crack Formation & Tension Stiffening

Sato & Vecchio model (2003)

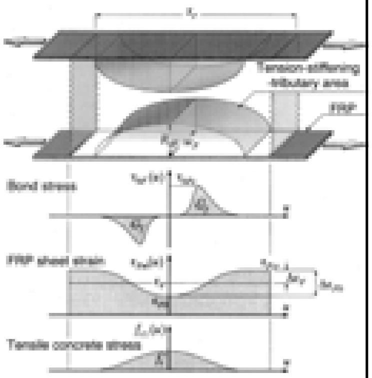
Tension-stiffening tributary area
FRP
Bond stress
FRP sheet strain
Tensile concrete stress

Load-Deflection Results

— Experiment

— — — Analysis

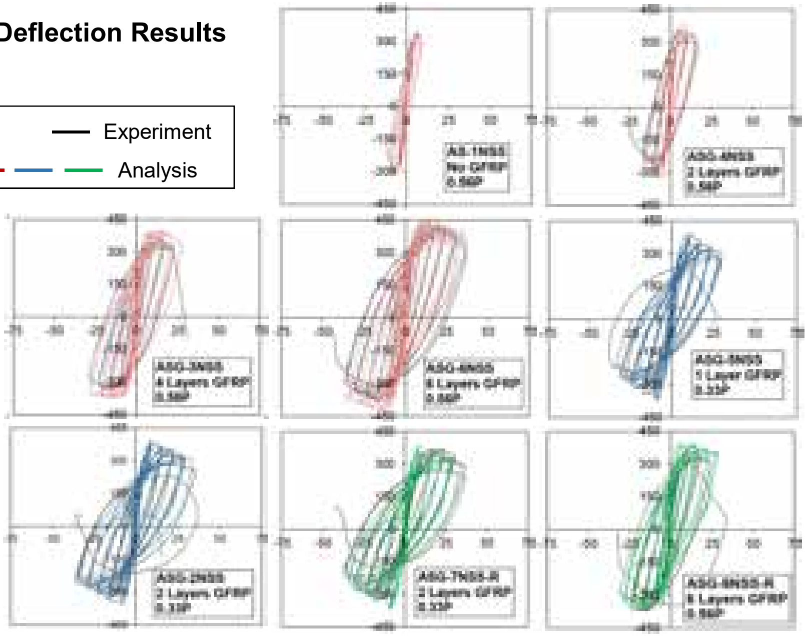

FRP-Repaired Structures: Component-Level Response

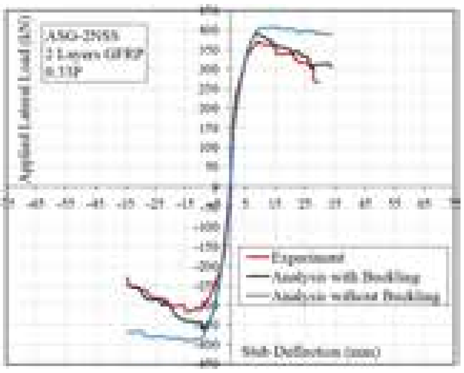

Influence of Bar Buckling

Influence of Initial Damage

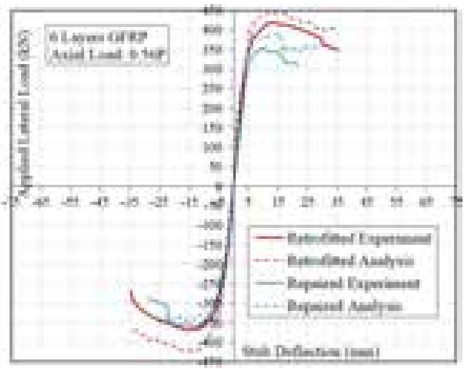

FRP-Repaired Structures: System-Level Response

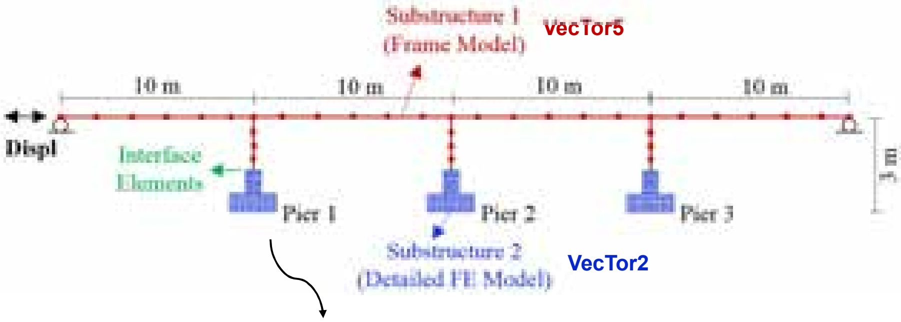
Substructure 1
(Frame Model)
10 m
10 m
10 m
10 m
Displ
Interface
Elements
Pier 1
Pier 2
Pier 3
3 m
Substructure 2
(Detailed FE Model)

VecTor5

VecTor2

RC pier

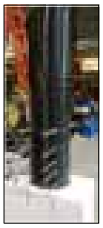

RC pier strengthened
with GFRP wraps

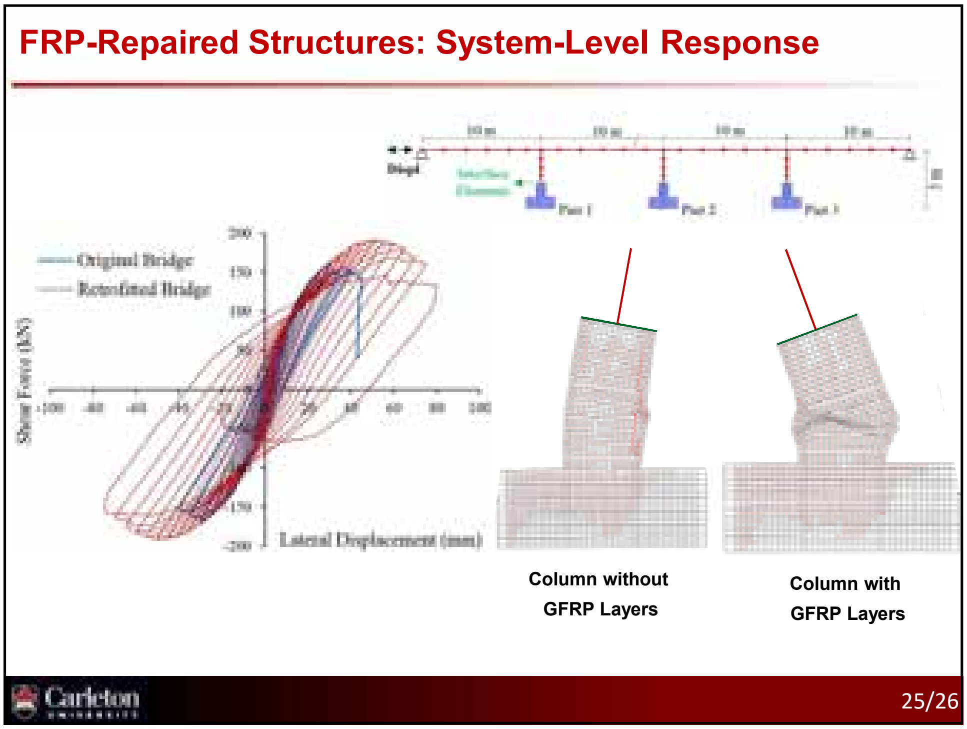

FRP-Repaired Structures: System-Level Response

Column without GFRP Layers

Column with GFRP Layers

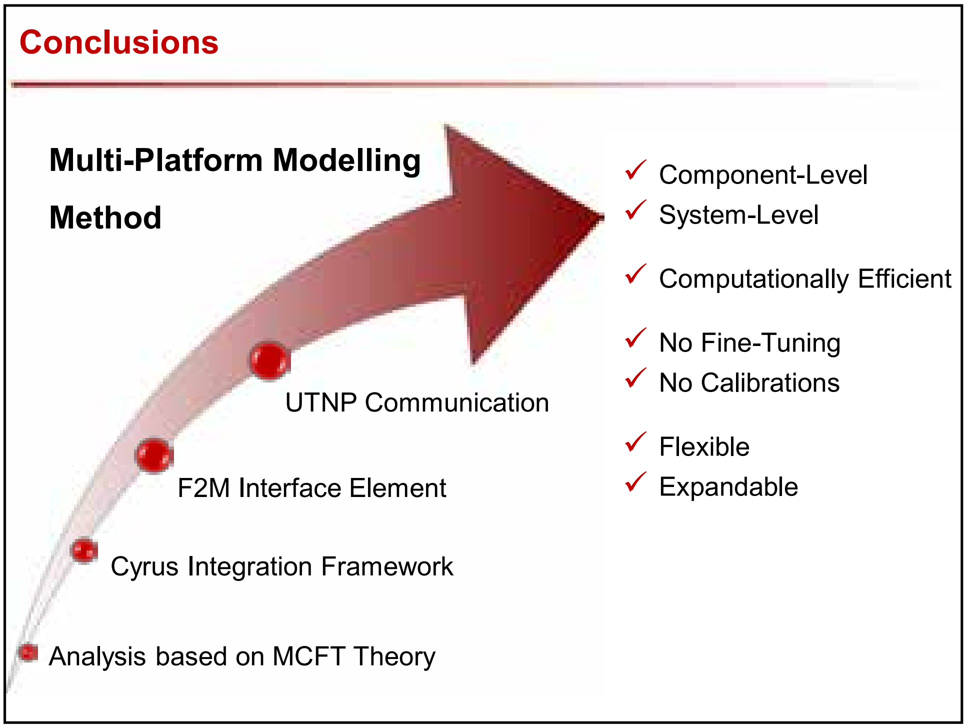

Conclusions

Multi-Platform Modelling Method

- Analysis based on MCFT Theory
- Cyrus Integration Framework
- F2M Interface Element
- UTNP Communication

✓ Component-Level
✓ System-Level

✓ Computationally Efficient

✓ No Fine-Tuning
✓ No Calibrations

✓ Flexible
✓ Expandable

Thank You

Current Research Directions

Application of **Multi-Platform Analysis** to advanced research areas:

1. Stochastic simulation

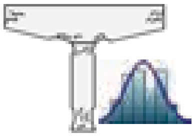

Stochastic simulation

2. Multi-hazard events

1906 San Francisco
earthquake-fire

Current Research Directions

Application of **Multi-Platform Analysis** to advanced research areas:

3. Modern concrete materials

96-meter long composite bridge, Germany
Miebach Engineering (Photo courtesy of:
Burkhard Walther Architekturfotografie)

4. Other strengthening Techniques
   - ✓ Textile reinforced concrete
   - ✓ Shape memory alloys

Application Example 2: Soil-Structure Interaction

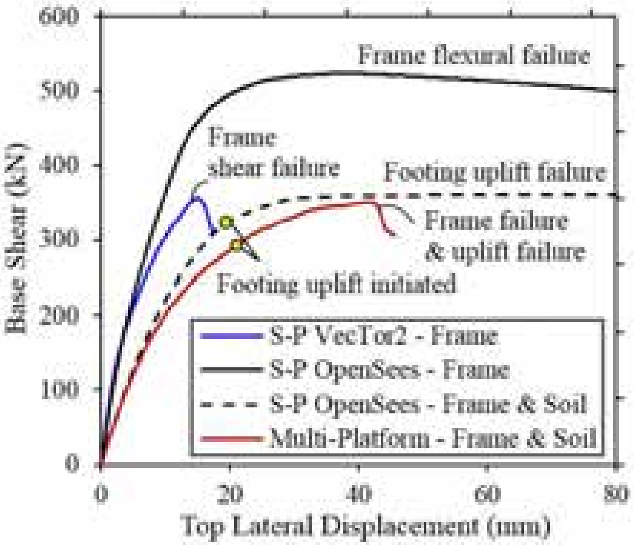

Application Example 2: Soil-Structure Interaction

- ❑ Elevation View
- ❑ Plan View

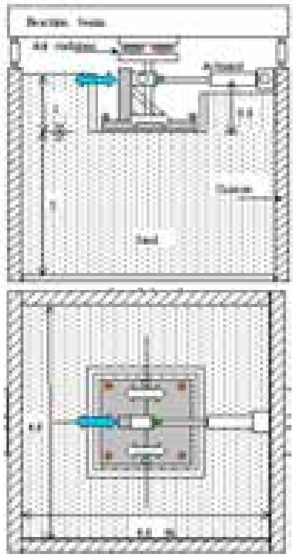

Negro et al. (2000)

Application Example 2: Soil-Structure Interaction

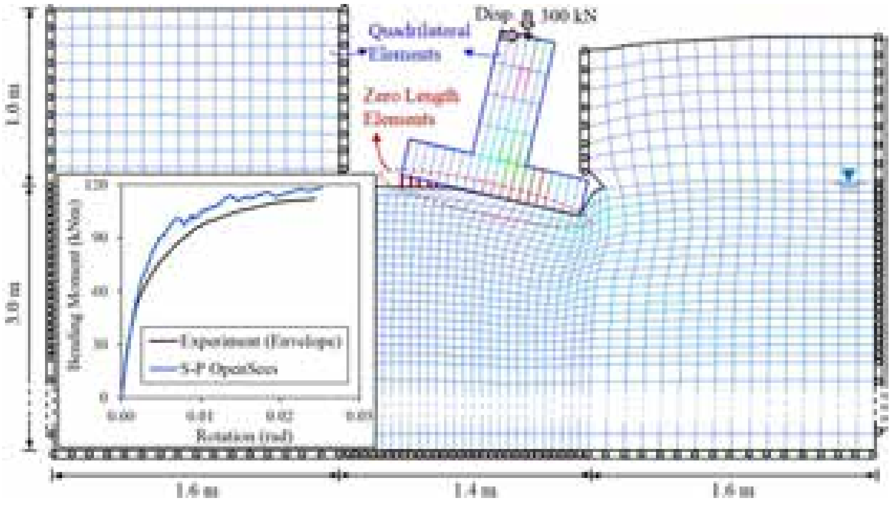
Disp
300 kN
Quadrilateral Elements
Zero Length Elements
1.0 m
3.0 m
Bending Moment (kNm)
120
90
60
30
0
0.00
0.01
0.02
0.03
Rotation (rad)
Experiment (Envelope)
S-P OpenSees
1.6 m
1.4 m
1.6 m

Modelling the Interface Between Sub-Models

❑ Rigid Links

- ⟐ Do not allow for transverse expansion.
- ⟐ Do not consider stress distribution.

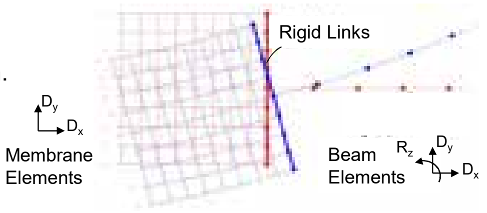
Rigid Links
D_y
D_x
Membrane Elements
Beam Elements
R_z
D_y
D_x

❑ Energy-Based Methods (McCune et al., 2000)

- ⟐ Uncouple effects of axial and shear stresses.
- ⟐ Limited to linear elastic modelling.

$$\underbrace{\int(\sigma_x U + \tau_{xy} V)dA}_{W_m} = \underbrace{Pu + Qv + M\theta}_{W_b}$$

Verification study: RC Beams (Vecchio & Shim, 2004)

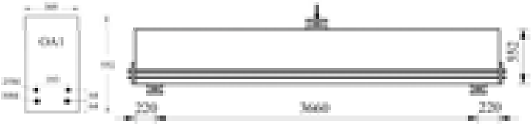
OA1
220
3660
220
552

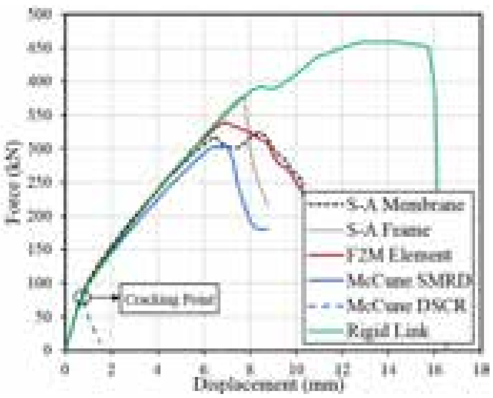

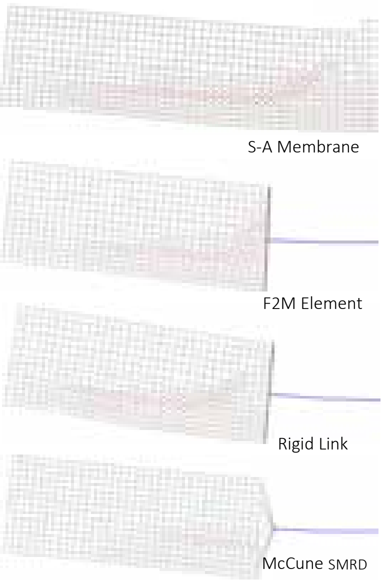
S-A Membrane
F2M Element
Rigid Link
McCune SMRD

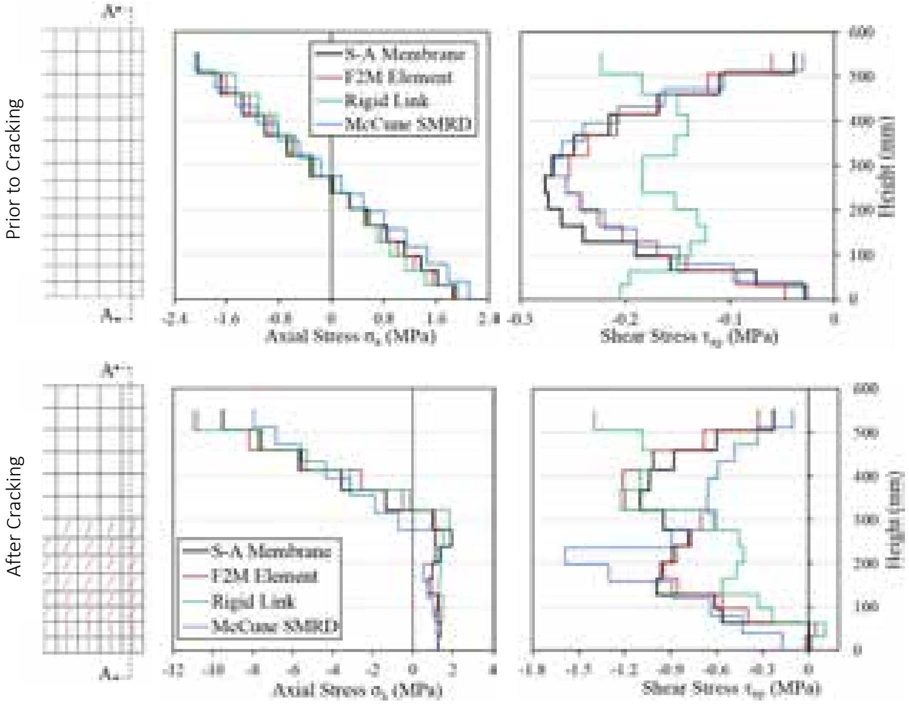

Application Example 2: Soil-Structure Interaction

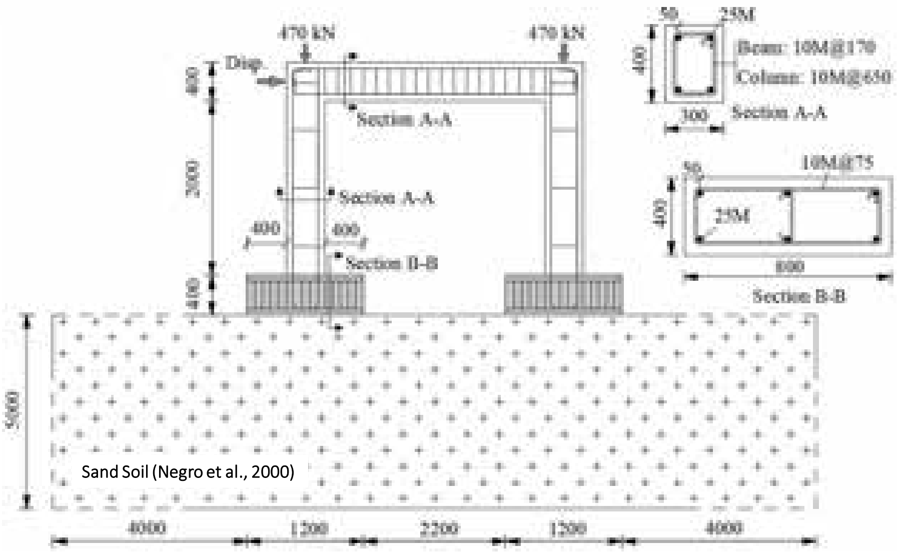
470 kN
470 kN
Disp.
Section A-A
Section A-A
Section B-B
400
2000
400
400
400
5000
50
25M
Beam: 10M@170
Column: 10M@650
400
300
Section A-A
50
10M@75
400
25M
800
Section B-B
4000
1200
2200
1200
4000

Sand Soil (Negro et al., 2000)

Solutions

1. Identify the application range of macro-models

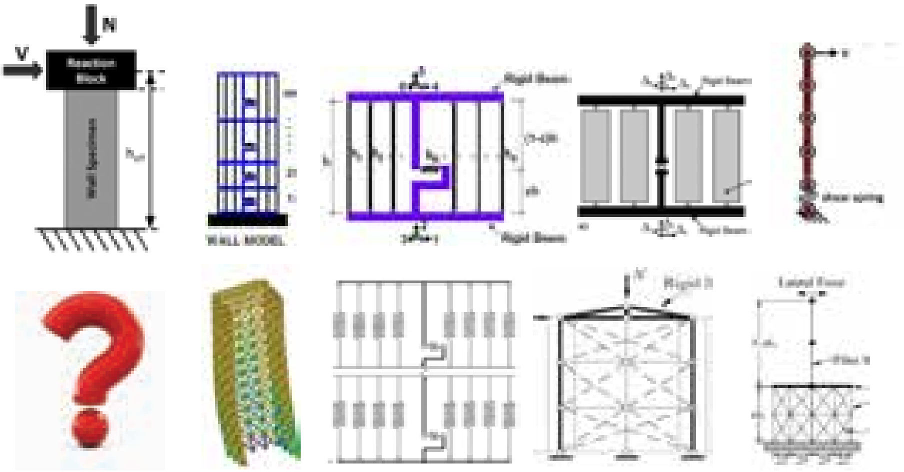
N
V
Reaction Block
Wall Specimen
WALL MODEL
Rigid Beam
Rigid Beam
shear spring
Lateral Force

Modelling the Interface Between Sub-Models

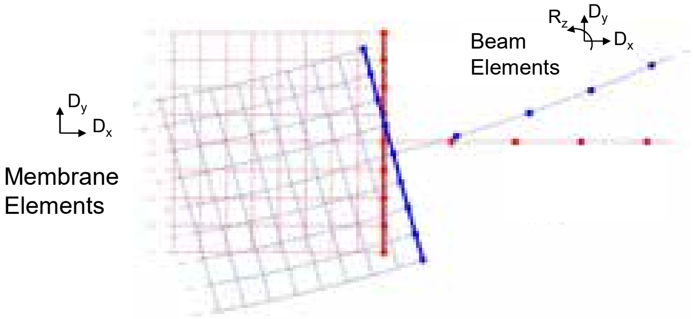
R_z
D_y
D_x
Beam Elements
D_y
D_x
Membrane Elements

Modelling the Interface Between Sub-Models

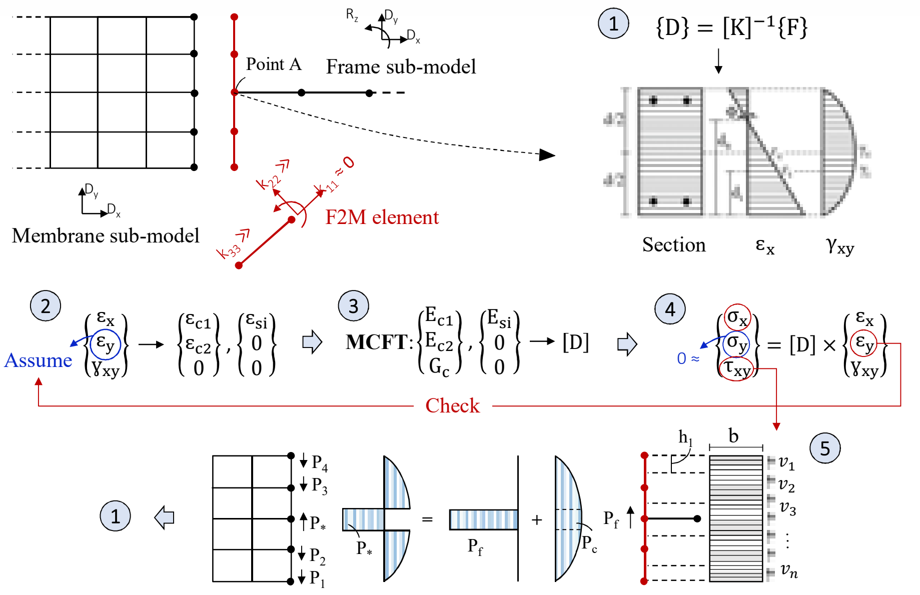
Membrane sub-model
D_y
D_x
Point A
Frame sub-model
R_z
F2M element
k_22 ≈
k_11 ≈ 0
k_33 ≈
1
{D} = [K]^−1{F}
Section
ε_x
γ_xy
2
Assume
ε_x, ε_y, γ_xy
ε_c1, ε_c2, 0
ε_si, 0, 0
3
MCFT:
E_c1, E_c2, G_c
E_si, 0, 0
[D]
4
0 ≈
σ_x, σ_y, τ_xy
= [D] ×
ε_x, ε_y, γ_xy
Check
5
h_1
b
v_1
v_2
v_3
v_n
P_f
1
P_4
P_3
P_*
P_2
P_1
P_*
=
P_f
+
P_c

OPTICAL FIBER SENSING WITH *N*-OTDR FOR STRUCTURAL DEFORMATION AND FAILURE MONITORING

By Dr. T.Y.P. Yuen, National Chiao Tung University

Abstract

Successful post-earthquake rehabilitation of structures and infrastructures is grounded on rapid locating the critical damage. Compared to point-sensors, distributed optical fibre sensing (DOFS) techniques offer the advantages of spatial continuous structural monitoring and does not require the prior knowledge of the critical locations needed for the sensor deployment. This talk presents the development of new measurement theory and algorithm to evaluate the structural deformation based on the large beam deflection and optical bend loss theories. In the experiment, the deformation events can be successfully evaluated from the optical bend loss and other OTDR trace parameters. The structural deformation and failure events can be pinpointed and the magnitudes can also be accurately evaluated with the proposed optical bend loss-deflection formula. The optical fibre sensing system has the potential to be integrated with different structural control devices and smart materials to develop the next generations of seismically intelligent and resilient engineered structures.

Keywords: distributed OFS, bend loss, large deformation, failure monitoring, POF, *v*-OTDR, smart engineered structures.

Biography

Dr Terry Y.P. Yuen is currently an Assistant Professor of Structural Engineering at National Chiao Tung University (NCTU) in Taiwan. His research covers topics in earthquake engineering and tall building structures. He has been the PI or co-PI of several international research projects funded by EPSRC (UK), TÜBİTAK (Turkey), and MOST (R.O.C). His research achievements have earned him several academic awards including the Structural Excellence R&D Award 2017 by the HKIE and IStructE (UK), and the Telford Premium 2014 by ICE (UK).

Optical Fibre Sensing with ν–OTDR

For Structural Deformation and Failure Monitoring

Terry YP YUEN, PhD
Dept. of Civil Engineering, NCTU

Canada
NRC CNRC
MOST 科技部

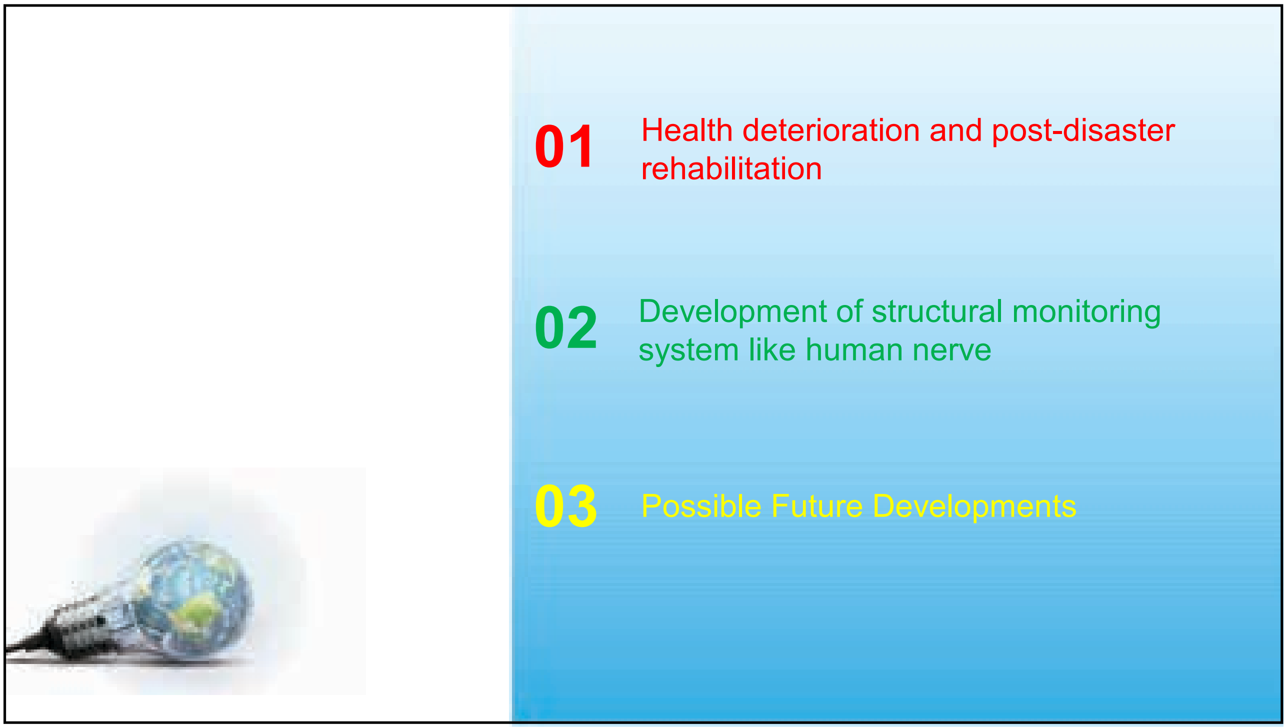

01 Health deterioration and post-disaster rehabilitation

02 Development of structural monitoring system like human nerve

03 Possible Future Developments

01 Health deterioration and post-disaster rehabilitation

Are our built-environment already protected with the technological advancements in structural engineering?

Seismic Retrofitting

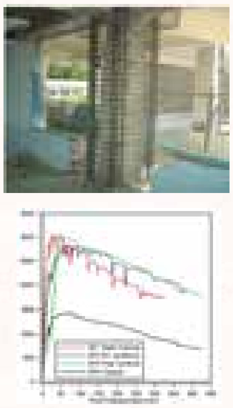

Hsiao et al., 2007

Engineered Cementitious Composites (ECC)

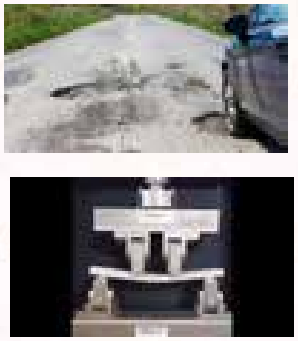

Victor Li (UMich)

Tuned Mass Damper

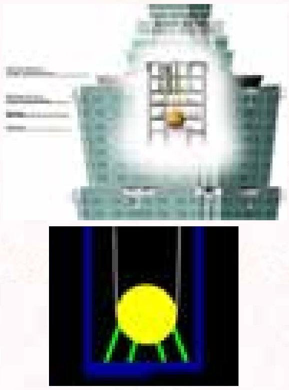

Tapei 101, Taiwan

Structural Isolation

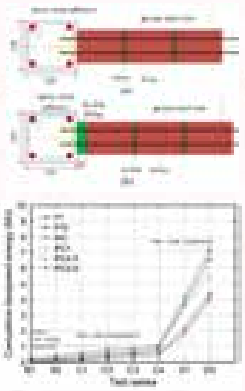

Yuen et al, 2018